Tracking of an omnidirectional targetwith a unicycle-like robot:control design and experimental results

Guillaume Artus, Pascal Morin, Claude Samson

INRIA

INSTITUT NATIONAL DE RECHERCHE EN INFORMATIQUE ET EN AUTOMATIQUE

Tracking of an omnidirectional target with a unicycle-like robot: control design and experimental results

Guillaume Artus — Pascal Morin — Claude Samson

N° 4849

Juin 2003

THÈME 4

ISSN 0249-6399 ISRN INRIA/RR--4849--FR+ENG

INRIA
SOPHIA ANTIPOLIS

Tracking of an omnidirectional target with a unicycle-like robot: control design and experimental results

Guillaume Artus , Pascal Morin , Claude Samson

Thème 4 — Simulation et optimisation
de systèmes complexes
Projet ICARE

Rapport de recherche n° 4849 — Juin 2003 — 31 pages

Abstract: A control strategy for tracking an omnidirectional target with a unicycle-like robot is proposed. An originality of the approach is that the target is allowed to move freely in the plane and perform motions which are not feasible by the nonholonomic robot. Control implementation involves the design of an estimator of the target's velocity, from visual and odometry measurements. Finally, simulation and experimental results are reported.

Key-words: practical stabilization, target tracking, nonholonomic robot, speed estimator

This work is supported by the European Project CyberCars

Unité de recherche INRIA Sophia Antipolis
2004, route des Lucioles, BP 93, 06902 Sophia Antipolis Cedex (France)
Téléphone : +33 4 92 38 77 77 —Télécopie : +33 4 92 38 77 65

Suivi d'une cible omnidirectionnelle par un robot unicycle: Synthèse de la commande et résultats expérimentaux

Résumé : Une stratégie de commande pour le suivi d'une cible omni-directionnelle avec un robot unicycle est présentée. Une originalité de cette approche est que la cible n'est pas contrainte dans ces mouvements et peut donc suivre des trajectoires non réalisables par le robot non-holonôme. La mise en œuvre pratique de la commande proposée passe par la réalisation d'un estimateur de la vitesse de la cible. Celui-ci est basé sur la fusion des données issues de la vision et de celles issues des mesures odométriques. Des résultats de simulation et d'expérimentation sont présentés.

Mots-clés : stabilisation pratique, suivi de cible, robot non-holonôme, estimateur de vitesse

Contents

Introduction

We consider the problem of tracking a vehicle — called *target* from now on — with a nonholonomic unicycle-like robot by using vision data acquired with an on-board camera. A distinctive feature of the present study is that no assumption is made on the target's motion so that, due to nonholonomic constraints on the robot which forbid instantaneous lateral motion, perfect tracking of the target is generically impossible. A practical situation which illustrates this problem arises when one is interested in making a robotic car automatically follow another car. This corresponds to a typical car-platooning application except that tracking has to be continued when the leader performs maneuvers that involve changes in the sign of its longitudinal velocity. To our knowledge, this type of problem has seldom been addressed in the literature. As a matter of fact, finding an adequate formulation of the control problem is not even straightforward in this case. Indeed, while following a leading vehicle with positive longitudinal velocity can be solved with classical control techniques, and is well documented in the robotics/automotive literature, what does tracking mean when the leader moves backward? A possible scenario consists in imagining a virtual frame attached behind the vehicle. The problem at hand then basically amounts to controlling the posture error between this frame and the robotic car's body. Zeroing this error all the time would correspond to perfect tracking. Stated in these terms, the control problem looks alike *trajectory tracking*, another much studied problem [5, 1]. There is however an important difference. In the trajectory tracking case, it is assumed that the reference trajectory is feasible, i.e. compatible with the kinematics of the controlled vehicle. In our case, this assumption does not hold because the velocity of the virtual frame has a lateral component which vanishes only when the vehicle moves along a straight line (as it is simple to verify). Since nonholonomy forbids such a lateral motion for the robotic car, perfect tracking of the virtual frame is usually not possible. Instead, some type of practical stabilization yielding, for instance, uniform ultimate boundedness of the tracking errors (in both position and orientation) has to be considered. The problem addressed in the present paper is a generalization, adapted to the case of a unicycle-type mobile robot, of the control problem evoked in the above example.

The control strategy here considered is based on the transverse function control approach [4] which provides a general framework for the design of control laws yielding practical stabilization for nonlinear controllable driftless systems submitted to additive perturbations. It is closely related to, and may be seen as an extension of, a control proposed in [2], where practical stabilization of feasible trajectories for a unicycle-type robot is studied. Estimation of the target's velocity is understandably useful for tracking purposes and improves the performance of the control scheme. The design of such an estimator, based on visual data — from which the relative configuration of the robot with respect to the target is reconstructed — and odometry measurements, is described in the paper. This is combined with the problem of filtering measurement noise on the reconstructed target/robot configuration.

The paper is organized as follows. Control models are introduced in Section 1. The control strategy is presented in Section 2. The target velocity estimator is presented in Section 3. Since mobile robots equations are nonlinear, the superposition principle of linear control theory does not apply. For this reason, a complementary analysis is needed to prove the stability of the proposed controller/estimator. It is conducted in Section 4. Various implementation issues are addressed in Section 5. Simulation and experimental results are reported in Sections 6 and 7 respectively. A few directions for future studies are pointed out in the Conclusion.

1 Modeling

Let us consider the three frames represented in Figure 1: $\mathcal{F}_0$ is a fixed frame, $\mathcal{F}_r$ is a frame attached to the unicycle, and $\mathcal{F}_t$ is a frame attached to the target. Let (x_r, y_r) denote the coordinates of $\overrightarrow{\mathrm{OP}_r}$ in $\mathcal{F}_0$ and α_r denote the angle between $\vec{\imath}_0$ and $\vec{\imath}_r$ (see Figure 1). The control inputs of the robot are the longitudinal velocity u_1 along the vector $\vec{\imath}_r$ of $\mathcal{F}_r$ and the angular velocity $u_2 = \dot{\alpha}_r$. With these notations, the kinematic equations of the unicycle, with respect to $\mathcal{F}_0$, are

$$\left\{ \begin{array}{rcl} \dot{x}_r &=& u_1 \cos\alpha_r \\ \dot{y}_r &=& u_1 \sin\alpha_r \\ \dot{\alpha}_r &=& u_2 \end{array} \right. \tag{1}$$

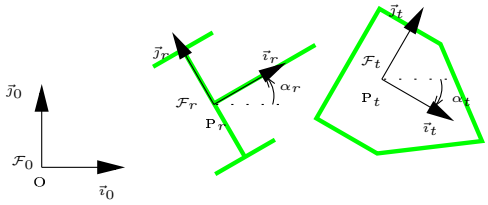

Figure 1: Configuration frames

For stabilization purposes, we want to describe the kinematics of the robot with respect to the target. Let (x_t, y_t) denote the coordinates of $\overrightarrow{\mathrm{OP}_t}$ in $\mathcal{F}_t$, and α_t denote the angle between $\vec{\imath}_0$ and $\vec{\imath}_t$. The two components of the velocity of P_t, expressed in the basis of the target frame, are denoted as a and b, and the target angular velocity is denoted as c, i.e.

$$\left\{ \begin{array}{rcl} \frac{d\overrightarrow{\mathrm{OP}_t}}{dt} &=& a\vec{\imath}_t + b\vec{\jmath}_t \\ \dot{\alpha}_t &=& c \end{array} \right. \tag{2}$$

We let

$$u_t = \begin{pmatrix} a & b & c \end{pmatrix}^T \tag{3}$$

If (x, y) denotes the coordinates of the position error vector between the robot and the target, expressed in the target frame $\mathcal{F}_t$, i.e. $\overrightarrow{\mathrm{P}_t\mathrm{P}_r} = x\vec{\imath}_t + y\vec{\jmath}_t$, and $\alpha = \alpha_r - \alpha_t$, one infers from (1) and (2) — see Appendix A for details — that

$$\left\{ \begin{array}{rcl} \dot{x} &=& u_1 \cos\alpha + cy - a \\ \dot{y} &=& u_1 \sin\alpha - cx - b \\ \dot{\alpha} &=& u_2 - c \end{array} \right. \tag{4}$$

System (4) represents the error system associated with the target tracking problem. It can be rewritten as

$$\dot{g} = u_1 b_1(g) + u_2 b_2 + b_0(g, u_t) \tag{5}$$

with $g = (x, y, \alpha)^T$ and

$$b_0(g, u_t) = (cy - a, -cx - b, -c)^T \tag{6}$$

$$b_1(g) = (\cos\alpha, \sin\alpha, 0)^T,\ b_2 = (0, 0, 1)^T \tag{7}$$

2 Control strategy

The control approach is based on the concept of *transverse functions* developed in [4]. In this section we only present the elements of the approach necessary for the considered application. Let us temporarily focus on System (5) without the drift term b_0, i.e.

$$\dot{g} = u_1 b_1(g) + u_2 b_2 \tag{8}$$

By definition, a bounded function $f : \mathbb{T} \longrightarrow G$ — with $\mathbb{T} \triangleq \mathbb{R}/2\pi\mathbb{Z}$ — is called a *transverse function* for System (8) if

$$\forall \theta \in \mathbb{T}, \quad \det H(\theta) \neq 0 \quad \text{with} \quad H(\theta) \triangleq \left(b_1(f(\theta)) \quad b_2 \quad -\frac{\partial f}{\partial \theta}(\theta) \right) \tag{9}$$

It is not difficult to show — see Appendix B — that for any $\varepsilon_1 > 0$ and any $\varepsilon_2 \in (0, \frac{\pi}{2}]$ the function f defined by

$$f(\theta) = \begin{pmatrix} \varepsilon_1 \sin\theta \\ \frac{\varepsilon_1 \varepsilon_2}{4} \sin 2\theta \\ \varepsilon_2 \cos\theta \end{pmatrix} \tag{10}$$

ensures the satisfaction of Condition (9). Transverse functions allow to introduce $\dot{\theta}$ as a new — virtual — control input for the system. In order to be more specific about this point, let us first recall a few basic definitions about Lie groups.

A Lie group G is a differentiable manifold equipped with a smooth group operation. The one here considered is $G = \mathbb{R}^2 \times \mathbb{T}$ endowed with the group operation $(g, g') \longmapsto gg'$ defined by

$$gg' = \begin{pmatrix} p + R(\alpha)p' \\ \alpha + \alpha' \end{pmatrix} \tag{11}$$

with $g = (p, \alpha)$, $g' = (p', \alpha')$, — p and $p' \in \mathbb{R}^2$ correspond to position vectors — and $R(\alpha)$ the rotation matrix of angle α. We denote by $e = (0, 0, 0)^T$ the unit element of the group.

It is well known, and straightforward to verify, that System (8) defines a left-invariant control system on G, i.e., for any solution $g(.)$ of (8) and any $g_0 \in G$,

$$\frac{d}{dt}(g_0 g(t)) = u_1 b_1(g_0 g(t)) + u_2 b_2$$

The following proposition provides the expression of a — dynamic — feedback law which ensures practical stability of the origin of System (5). In this proposition, d stands for the differential, r_h and l_h denote the right and left translations by h respectively, i.e. $r_h(g) = gh$ and $l_h(g) = hg$.

Proposition 1 *Let $\mathcal{U} \subset G$ denote a neighborhood of e, and $f : \mathbb{T} \longrightarrow \mathcal{U}$ a transverse function. Let $\bar{u} \triangleq (u_1, u_2, \dot{\theta})^T$. Consider the following dynamic feedback law*

$$\bar{u} = -H(\theta)^{-1} \left[dl_z(g)\, b_0(g, u_t) + dr_g(z)\, Kz \right] \tag{12}$$

with

$$\begin{aligned} dl_z(g) &= \begin{pmatrix} R(\varepsilon_2 \cos\theta - \alpha) & 0 \\ 0 & 1 \end{pmatrix} \\ dr_g(z) &= \begin{pmatrix} I_2 & R(\varepsilon_2 \cos\theta - \alpha) \begin{pmatrix} -y \\ x \end{pmatrix} \\ 0 & 1 \end{pmatrix} \\ z \triangleq f(\theta) g^{-1} &= f(\theta) - \begin{pmatrix} R(\varepsilon_2 \cos\theta - \alpha) \begin{pmatrix} x \\ y \end{pmatrix} \\ \alpha \end{pmatrix} \end{aligned} \tag{13}$$

Applying this control to (5) *yields* $\dot{z} = Kz$. *Therefore, if* K *is a Hurwitz stable matrix,* $\bar{u}$ *ensures the practical stabilization of* $g = e$ *in the sense that the set* $f(\mathbb{T})$ *is exponentially stable for the closed-loop system* (5)–(12). *In particular, if* $K = -diag\{k_1, k_2, k_3\}$ *with* $k_{1,2,3} > 0$, *any solution* $g(.)$ *of* (5) *such that* $|z_3(0)| = |\alpha(0) - f_3(\theta(0))| < \pi$ *converges exponentially to* $f(\mathbb{T})$.

Since $f(\theta)$, as given by (10), tends to zero when the parameters ε_1 and ε_2 tend to zero, $\|g(t)\|$ is ultimately bounded by a number which can be rendered as small as desired by choosing these parameters small enough (but different from zero). Moreover, this bound is *independent* of the target's motion. Note, however, that a small value for this bound may not be necessary, nor desirable, in practice.

Remark: The convergence condition $|z_3(0)| = |\alpha(0) - f_3(\theta(0))| < \pi$ in Proposition 1, comes from the fact that there exists no continuous *global* stabilizer of any element of $\mathbb{T}$.

3 Estimator design

The knowledge of the target velocity u_t is needed to implement the feedback law (12). Since this velocity is not directly measured, an estimator is built from measurements of the tracking error $g(t)$. These measurements are themselves obtained from visual data via standard geometric calculations which will not be detailed here. The estimator is designed to also provide filtered values of the measurements of $g(t)$. This is important for our experiments because the data delivered by the on-board camera happens to be quite noisy.

In the first place, a model of the target dynamics has to be chosen. When the target velocity, with respect to the fixed frame, is constant, we infer from (2) that

$$\left\{ \begin{array}{rcl} \dot{a} & = & cb \\ \dot{b} & = & -ca \\ \dot{c} & = & 0 \end{array} \right.$$

In order to account for possible variations of this velocity we will use the following model

$$\left\{ \begin{array}{rcl} \dot{a} & = & cb + v_a \\ \dot{b} & = & -ca + v_b \\ \dot{c} & = & v_c \end{array} \right. \tag{14}$$

where v_a, v_b, and v_c are *bounded* acceleration inputs.

The robot velocities u_1 and u_2 are assumed to be measured via odometry. Note that, for estimation purposes, odometry measurements are usually preferred to *desired* control values, as specified by the control law (12), because they often describe the reality more accurately. However, odometry information is slightly corrupted by noise and it is further degraded by signal processing induced delays. Undetected slippage of the actuating wheels may also account for episodic discrepancies between the odometry measurements and the actual velocity of the robot body. Let u_1^o and u_2^o denote these measurements. The above considerations lead us to rewrite System (4) as

$$\left\{ \begin{array}{rcl} \dot{x} & = & (u_1^o + v_1)\cos\alpha + cy - a \\ \dot{y} & = & (u_1^o + v_1)\sin\alpha - cx - b \\ \dot{\alpha} & = & (u_2^o + v_2) - c \end{array} \right. \tag{15}$$

where v_1 and v_2 can be interpreted as small bounded perturbations associated with odometry measurements.

Measurements of $p = (x, y)^T$ and α, obtained from visual data, are denoted as p^v and α^v. Due to the imperfection of these measurements we have

$$p^v = p + v_p = p + (v_x, v_y)^T \tag{16a}$$

$$\alpha^v = \alpha + v_\alpha \tag{16b}$$

where v_x, v_y, and v_α represent bounded measurement errors. In the forthcoming analysis, v_M denotes the maximum amplitude over all the terms v_{index} that we have introduced.

Now, the six equations in the models (14) and (15) can be regrouped and rewritten as

$$\dot{X}_p = A_p(c)X_p + U_p(\alpha) + V_p \tag{17a}$$

$$\dot{X}_\alpha = A_\alpha X_\alpha + U_\alpha + V_\alpha \tag{17b}$$

with

$$\begin{array}{l} X_p = (x, y, a, b)^T = (p^T, a, b)^T,\ X_\alpha = (\alpha, c)^T \\ U_p = (u_1^o \cos\alpha, u_1^o \sin\alpha, 0, 0)^T,\ U_\alpha = (u_2^o, 0)^T \\ V_p = (v_1 \cos\alpha, v_1 \sin\alpha, v_a, v_b),\ V_\alpha = (v_2, v_c)^T \\ A_p(c) = \begin{pmatrix} 0 & c & -1 & 0 \\ -c & 0 & 0 & -1 \\ 0 & 0 & 0 & c \\ 0 & 0 & -c & 0 \end{pmatrix},\ A_\alpha = \begin{pmatrix} 0 & -1 \\ 0 & 0 \end{pmatrix} \end{array} \tag{18}$$

The linear dynamics of X_α and the nonlinear ones of X_p, appear clearly in (17). We propose an estimator in the following form:

$$\dot{\hat{X}}_p = A_p(\hat{c})\hat{X}_p + U_p(\hat{\alpha}) + D_p(p^v - \hat{p}) \tag{19a}$$

$$\dot{\hat{X}}_\alpha = A_\alpha \hat{X}_\alpha + U_\alpha + D_\alpha(\alpha^v - \hat{\alpha}) \tag{19b}$$

where D_p and D_α are matrix-valued gains, chosen in accordance with the stability analysis summarized in the following proposition.

Proposition 2 *Let*

$$D_p = \begin{pmatrix} \lambda_p & 0 \\ 0 & \lambda_p \\ -\beta_p & 0 \\ 0 & -\beta_p \end{pmatrix},\ D_\alpha = \begin{pmatrix} \lambda_\alpha \\ -\beta_\alpha \end{pmatrix} \tag{20}$$

with $\lambda_p, \beta_p, \lambda_\alpha, \beta_\alpha > 0$, and denote the estimation error by $\tilde{X} \triangleq (X_p - \hat{X}_p, X_\alpha - \hat{X}_\alpha)$. If the robot velocities u_1, u_2, and X_p are bounded functions of time, then $\|\tilde{X}(t)\| \leq c_1 v_M + c_2 e^{-\gamma t}\|\tilde{X}(0)\|$ for some constants $c_1, c_2, \gamma > 0$.

The proof of Proposition 2 is given in Appendix C.1.

A way to further specify the estimator's gains in (20) consists in assuming that all terms of the form v_{index} are uncorrelated zero-mean white noises with given covariances and calculating the corresponding steady-state optimal Kalman gains. Let us denote by $\omega_{index} = \mathrm{E}[v_{index}^2]$ the covariance of v_{index}. The linear subsystem (17b) associated with the orientation variable X_α poses no difficulty for the calculation of the optimal gain D_α (see, for instance, [3, Sec. 4.4], for an exposition of the Kalman filter). As for Subsystem (17a), a difficulty arises from the nonlinearity of this system. It is circumvented by assuming that c is constant in $A_p(c)$, and $v_1 = 0$ in V_p. One obtains after calculations presented in Appendix C.2:

Lemma 1 *If $\omega_2 \ll \sqrt{\omega_c \omega_\alpha}$, the steady-state optimal Kalman gain D_α associated with* (16b)–(17b) *is given by* (20) *with*

$$\lambda_\alpha \approx \sqrt{2}(\omega_c/\omega_\alpha)^{\frac{1}{4}},\quad \beta_\alpha \approx (\omega_c/\omega_\alpha)^{\frac{1}{2}} \tag{21}$$

Similarly, the steady-state optimal Kalman gain D_p associated with (16a)-(17a)*, when c is constant, $\omega_x = \omega_y$, $\omega_a = \omega_b$, and $\omega_1 = 0$, is given by (20) with*

$$\lambda_p = \sqrt{2}(\omega_a/\omega_x)^{\frac{1}{4}},\quad \beta_p = (\omega_a/\omega_x)^{\frac{1}{2}} \tag{22}$$

4 Controller/estimator stability

In this section, the two following assumptions are made:
Assumptions:

1. The target velocity is bounded.
2. The stabilizer gain matrix K — see Equation (12) — is block diagonal, i.e.,

$$K = \begin{pmatrix} K_p & 0 \\ 0 & k_\alpha \end{pmatrix} \tag{23}$$

with K_p a 2×2 matrix.

The control (12) of Section 2 is a function of g, u_t, and θ (since $z = f(\theta)g^{-1}$), i.e. $\bar{u} = \bar{u}(g, u_t, \theta)$. The estimator (19) of Section 3 provides estimated values $\hat{g}$ and $\hat{u}_t$ for g and u_t. Since visual measurements g^v of g are also available, one can use either $\hat{g}$ or g^v, or a suitable combination of both, in the control calculation. In particular, whenever $|\hat{g}_i - g_i^v| \geq 2v_M$, g_i^v provides an estimation of g_i which is better than $\hat{g}_i$. The following proposition establishes the joint stability of the controller/estimator.

Proposition 3 *Consider the control law* (12) *of Section 2 with K block diagonal negative and the estimator* (19) *of Section 3. Assume that the target velocity u_t is bounded, and that the feedback $\bar{u}(g^e, \hat{u}_t, \theta)$ is applied to System* (5)*, with g^e equal to either $\hat{g}$ or g^v, or any other estimation of g such that $\|g^e - g\| \leq \gamma v_M$ for some constant γ. Then, if v_M is small enough, the closed-loop system* (5)–(12) *together with the estimator* (19) *is stable and $\lim_{t \longrightarrow \infty}(\|z(t)\| + \|\tilde{X}(t)\|) \leq C v_M$ for some constant C.*

The proof of Proposition 3 is given in Appendix D.

In practice, the choice $g^e = g^v$ will typically be preferred to $g_e = \hat{g}$ when abrupt variations of the target velocity, or slippage of the actuating wheels, prevent the estimator (19) from performing well. The opposite choice will normally provide a better estimation for g when the target velocity is known to be constant, or almost constant. This choice will therefore often be based on extra information about the nature and amplitude of the perturbation terms v_{index}. This information may either be available in advance or gathered online by using other sensors.

5 Implementation issues

In this section, T denotes the sampling period (corresponding to the video rate of the camera, for instance) and $X[k] = X(kT)$ is the value of X at time kT ($k \in \mathbb{N}$). The control vector is periodically updated and kept constant between two sampling time instants.

5.1 Control discretization

5.1.1 Estimator

The estimator (19) is implemented in discrete time via a two-steps prediction/correction computation. With $\hat{c}$ and $\hat{\alpha}$ kept constant on $[kT, (k+1)T)$, System (19) is linear on this interval. Analytic integration of this linear system yields — see Appendix E.1 — the following prediction of $X[k+1]$ just before using the visual measurements at time $(k+1)T$:

$$\hat{X}_p^-[k+1] = \begin{pmatrix} R_c[k] & -TR_c[k] \\ 0 & R_c[k] \end{pmatrix} \hat{X}_p[k] + \begin{pmatrix} R_\alpha[k+1]\Delta p_r^o[k+1] \\ 0 \end{pmatrix} \tag{24a}$$

$$\hat{X}_\alpha^-[k+1] = \begin{pmatrix} 1 & -T \\ 0 & 1 \end{pmatrix} \hat{X}_\alpha[k+1] + \begin{pmatrix} \Delta\alpha_r^o[k+1] \\ 0 \end{pmatrix} \tag{24b}$$

with $R_c[k]$ the rotation matrix of angle $-T\hat{c}[k]$, $R_\alpha[k+1]$ the rotation matrix of angle $\hat{\alpha}^-[k+1]$, $\Delta p_r^o[k+1]$ the robot's displacement in position, measured by odometry, between times kT and $(k+1)T$ expressed in the frame $\mathcal{F}_r$ at time $(k+1)T$, and $\Delta\alpha_r^o[k+1] = \alpha_r[k+1] - \alpha_r[k]$ the change in orientation of the robot between times kT and $(k+1)T$, also measured by odometry. The estimation of $X[k+1]$, which uses visual measurements at time $(k+1)T$, is then given by

$$\hat{X}_p[k+1] = \hat{X}_p^-[k+1] + TD_p\left(p^v[k+1] - \hat{p}^-[k+1]\right) \tag{25a}$$

$$\hat{X}_\alpha[k+1] = \hat{X}_\alpha^-[k+1] + TD_\alpha\left(\alpha^v[k+1] - \hat{\alpha}^-[k+1]\right) \tag{25b}$$

5.1.2 Transverse functions

The control function (12) depends on the variable θ. In fact, one easily verifies that it depends on $\eta_1 = \sin\theta$ and $\eta_2 = \cos\theta$. Since $\dot{\eta}_1 = \dot{\theta}\eta_2$ and $\dot{\eta}_2 = -\dot{\theta}\eta_1$, the discretization of η_1 and η_2, when $\dot{\theta}$ is constant on $[kT, (k+1)T)$, yields

$$\Psi[k+1] = R(-T\dot{\theta}[k])\Psi[k] \tag{26}$$

with $\Psi[k] = (\eta_1[k], \eta_2[k])^T$ and $R(-T\dot{\theta}[k])$ the rotation matrix of angle $-T\dot{\theta}[k]$. In order to guarantee the numerical stability of $\|\Psi[k]\|^2 - 1 = 0$, the following modified version of (26) is implemented:

$$\Psi[k+1] = \left(1 + \beta\left(\|\Psi[k]\|^2 - 1\right)\right) R(-T\dot{\theta}[k])\Psi[k] \tag{27}$$

Numerical stability is ensured, providing that $\beta \in (-1, 0)$ (see Appendix E.2).

5.2 Control initialization

When implementing (27), an initial value $\Psi(0)$ or, what is the same, an initial value $\theta(0)$ must be chosen. We choose $\theta(0)$ to minimize $|z_3(0)| = |\varepsilon_2 \cos\theta(0) - \alpha(0)|$. Namely if $|\alpha(0)| \leq \varepsilon_2$, $\theta(0)$ is chosen to obtain $\varepsilon_2 \cos\theta(0) = \alpha(0)$ (note that in this case, if K in (12) is diagonal, Proposition 1 implies that $z_3(t) = 0$ for all t). This choice limits transient oscillations when the target is fixed. If $|\alpha(0)| > \varepsilon_2$, we let $\theta(0) = k\pi$ with k such that $\cos\theta(0)$ and $\alpha(0)$ have the same sign. When $|\alpha(0)| \leq \varepsilon_2$, the sign of $\theta(0)$ has also to be chosen. In order to explain our choice, let us assume for example that the target is moving along its axis $\vec{\imath}_t$, i.e. $b = c = 0$ in Equation (3), with a constant speed a. Then, there exist stable equilibrium values of θ on the zero-dynamics $z \equiv 0$. These equilibrium values θ_e are given — see Appendix F for details — by

$$\theta_e = -sign(a)\frac{\pi}{2}$$

By (13), on the zero dynamics $z \equiv 0$, we have $z_1 = f_1(\theta) - x = 0$ so that, by (10), $x = f_1(\theta) = \varepsilon_1 \sin\theta$. Therefore, along these linear motions of the target, x should asymptotically converge to $\varepsilon_1 \sin\theta_e = -\varepsilon_1 sign(a)$ — i.e. the robot will stay behind the target for positive velocities of the latter, and ahead of it in the opposite case. Since, for these stable equilibria, $x = \varepsilon_1 \sin\theta_e$, x and θ have the same sign. Therefore, in order to minimize the initial "distance" to these potential equilibria, the sign of $\theta(0)$ is chosen equal to the one of $x(0)$. Simulation results, like those presented on Figure 2, and experimental results confirm the practical correctness of this strategy.

There still remains to consider the case $x(0) = 0$, for which $sign(x(0))$ is not defined. In this case, it follows again from (10), (13), and the fact that $\theta(0)$ has been chosen so that $z_3(0) = 0$, that

$$z(0) = \begin{pmatrix} \varepsilon_1 \sin\theta(0) \\ -y(0) + \frac{\varepsilon_1}{2}\alpha(0)\sin\theta(0) \\ 0 \end{pmatrix}$$

In this case, the sign of $\theta(0)$ is chosen so as to minimize $|z(0)|$, i.e. $sign(\theta(0)) = sign(\alpha(0)y(0))$ if $y(0)\alpha(0) \neq 0$. If $y(0)\alpha(0) = 0$, we arbitrarily choose $\theta(0)$ negative.

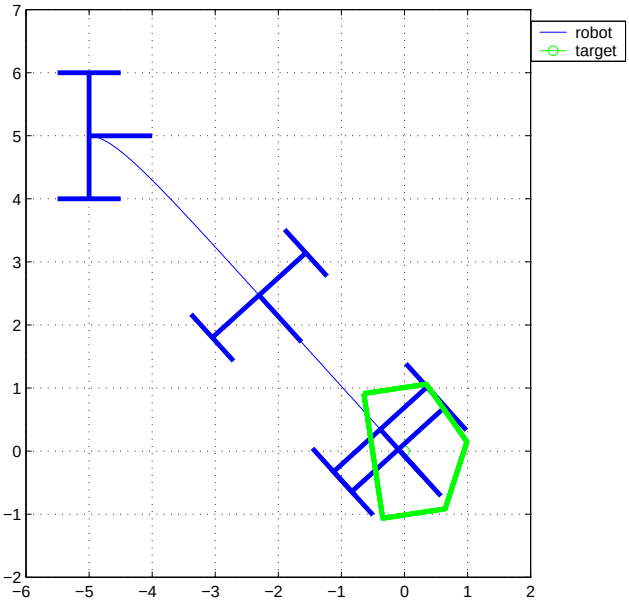

(a) Choice 1: $sign(\theta(0)) = sign(x(0))$

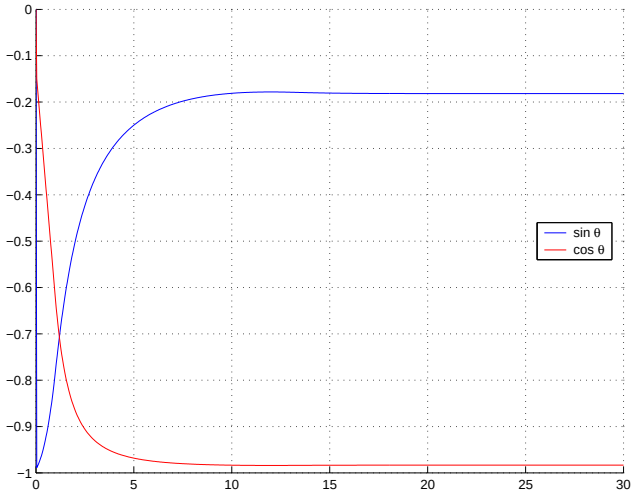

(b) $\sin\theta$ and $\cos\theta$

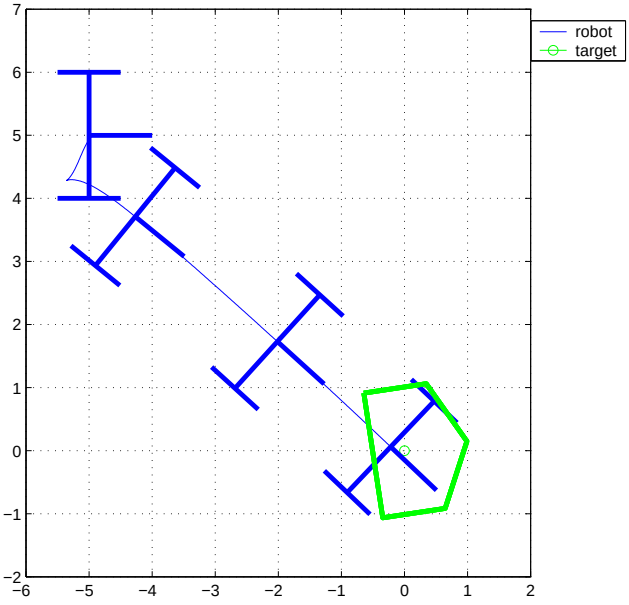

(c) Choice 2: $sign(\theta(0)) = -sign(x(0))$

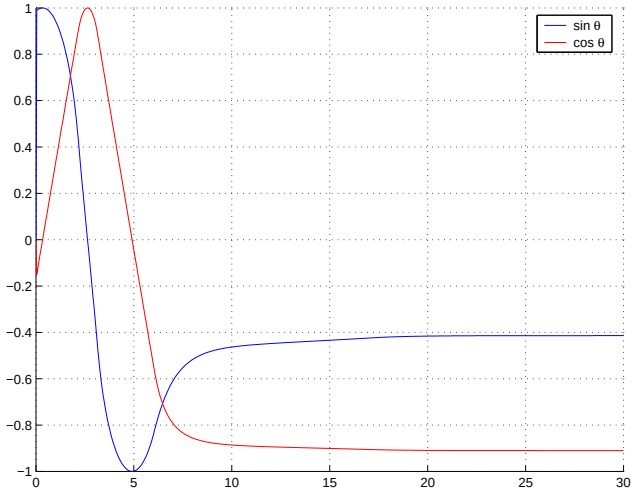

(d) $\sin\theta$ and $\cos\theta$

Figure 2: Influence of the choice of $\theta(0)$ on the transient behavior

5.3 Input saturation

In order to take into account physical velocity limitations $|u_i| \leq u_{i,\max}$ $(i = 1, 2)$, the control $\bar{u}$ in (12) is "rescaled" to $\bar{u}_{new} = \tau^{-1}\bar{u}$ with $\tau = \max\{1, |u_i|/u_{i,\max}, i = 1, 2\}$. One can show that this rescaling does not prevent the convergence of z to zero, provided that the target maintains its velocity within the range for which perfect tracking — in the sense of zeroing the vector z — remains possible. Moreover, in the case where the target is motionless the geometric path followed by the robot is not modified by this rescaling.

6 Simulation results

In the noiseless simulation results presented in Figures 3-5, the matrix K in (12) is given by $K = -0.5\mathrm{I}_3$ with I_3 the identity matrix. The transverse function (10) is used with $\varepsilon_1 = 0.5$ and $\varepsilon_2 = 1$. The observer gains are defined by (20) with $\lambda_\alpha = \lambda_p = \beta_\alpha = \beta_p = 2$. The estimation $g^e = \hat{g}$ is used in the controller. The discretized version of the control law (see Section 5) is applied, with the sampling period $T = 40$ms.

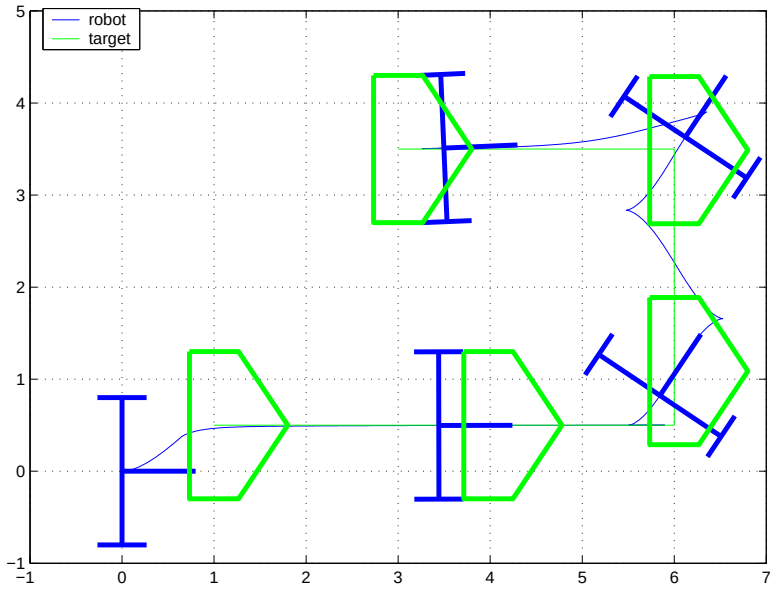

Figure 3: Cartesian motion: robot and target

The target motion is as follows. Initially, the target's posture correspond to $(x_r, y_r) = (1, 0.5)$ and $\alpha_r = 0$. After 10s, the target moves with constant longitudinal speed along the fixed axis $\vec{\imath}_0$. During this motion, θ tends to $\theta_0 = -\frac{\pi}{2}$, so that (x, y, α) tends to $(-\varepsilon_1, 0, 0)$ — See Appendix F for details. For $t \in]20s, 30s]$, it is motionless. For $t \in]30s, 40s]$, the target moves laterally along the axis $\vec{\jmath}_0$. This corresponds to a non-feasible motion for the robot. For $t \in]40s, 50s]$ the target moves backward with constant longitudinal speed along the axis $\vec{\imath}_0$, and is motionless thereafter. One can observe from Figure 5 that z sometimes departs from zero. This corresponds to abrupt changes in the target's velocity yielding transient estimation errors which in turn reflect on the control performance.

7 Experimental results

The proposed control law has also been tested experimentally on ANIS: a unicycle-like robot carrying a 6-d.o.f manipulator arm with a CCD camera at its extremity. The measurements g^v of the robot's

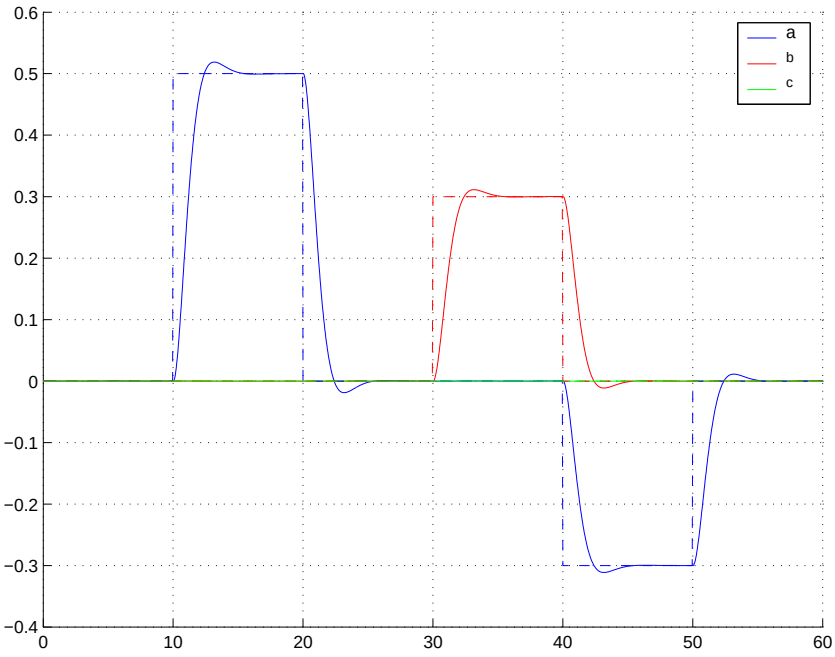

Figure 4: Estimated target speed

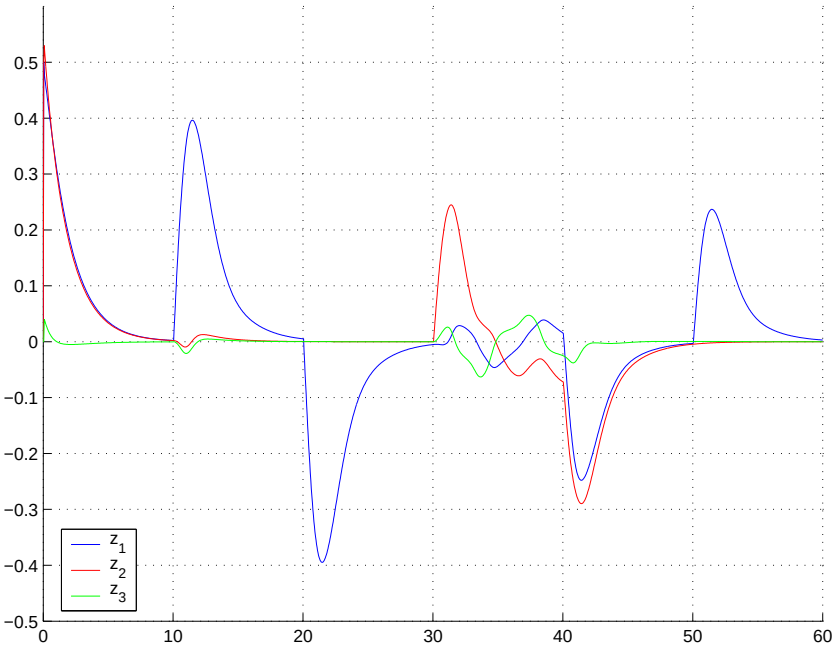

Figure 5: $z \stackrel{\Delta}{=} f(\theta)g^{-1}$

configuration with respect to the target are reconstructed from visual data. More details on the experimental set-up can be found in [6]. In the absence of sensors capable of providing measurements of the target's absolute position and velocity, only experimental results with a fixed target are reported. They illustrate the influence of the ε_i's on the robot behavior: $\varepsilon_2 = 0.3$ for Figure 6, $\varepsilon_2 = 1$ for Figure 8. In both cases, $\varepsilon_1 = 0.5$, and the gain matrices are those used for the simulation results of Section 6.

The cartesian trajectory shown in Figure 6(a) and 8(a) are obtained by using the estimation $g^e = \hat{g}$ of g. Therefore they do not depict the actual trajectories of the physical robot exactly, but are only approximations of these trajectories. For comparison purposes, noiseless simulation results with the same initial conditions and control parameters are also reported.

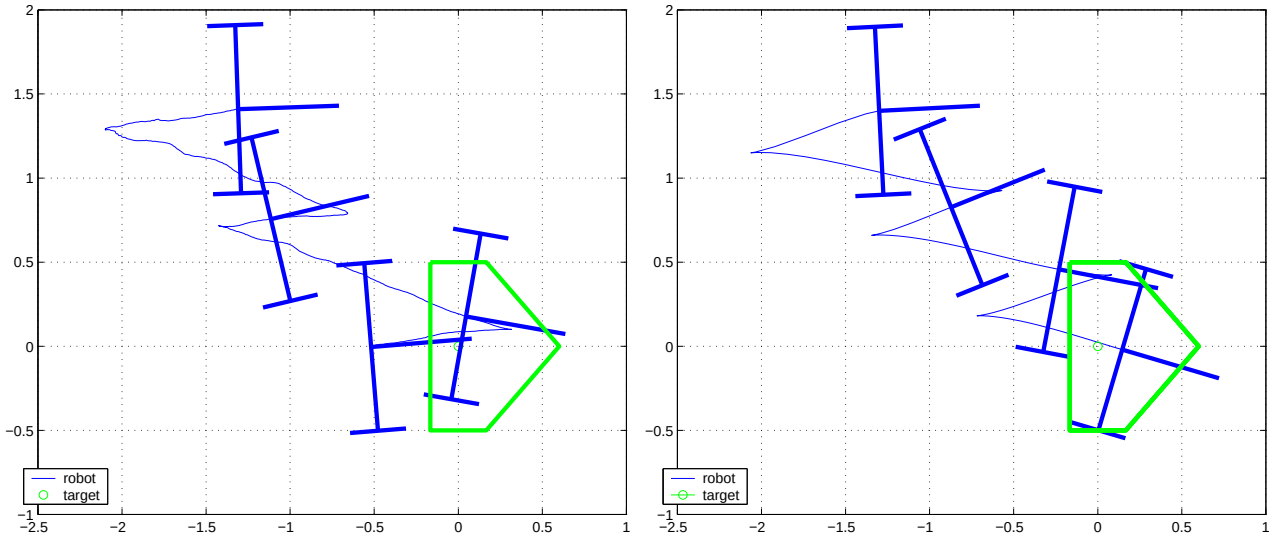

(a) Estimated trajectory during experimentation (b) Simulation

Figure 6: Cartesian motion of the robot $\varepsilon_2 = 0.3$

Some differences between experimental and simulation results can be observed from figures 6(a) and 6(b). They reflect the effects of various simplifications made in the considered model of the robot, control actuators, and sensors (friction, wheels' slippage, unmodeled dynamics, low-level control loops, delays resulting from visual data processing...). In particular, the final posture of the physical robot is significantly different from the one obtained in simulation. Two main combined reasons account for this:

1. the variable θ is not actively controlled so that the convergence of $z = f(\theta)g^{-1}$ to zero merely implies that g tends to $f(\theta)$ with no specific constraint upon the asymptotic value of θ,

2. the values chosen for ε_1 and ε_2 are not small so that $f(\theta_1)$ can be significantly different from $f(\theta_2)$ when $\|\theta_1 - \theta_2\|$ is not small.

The convergence to zero of the three components of $z = f(\theta)\hat{g}^{-1}$ is shown in Figure 7(a) and 7(b), when $\varepsilon_2 = 0.3$. Note that it is not exponential at the beginning of the motion, as a consequence of the saturations imposed on the control inputs (See Section 5.3).

Note also that discrepancies in the evolution of $\theta(t)$ are not systematic either, as this is illustrated by Figures 8(a) and 8(b) which show a better correspondence between simulation and experimentation.

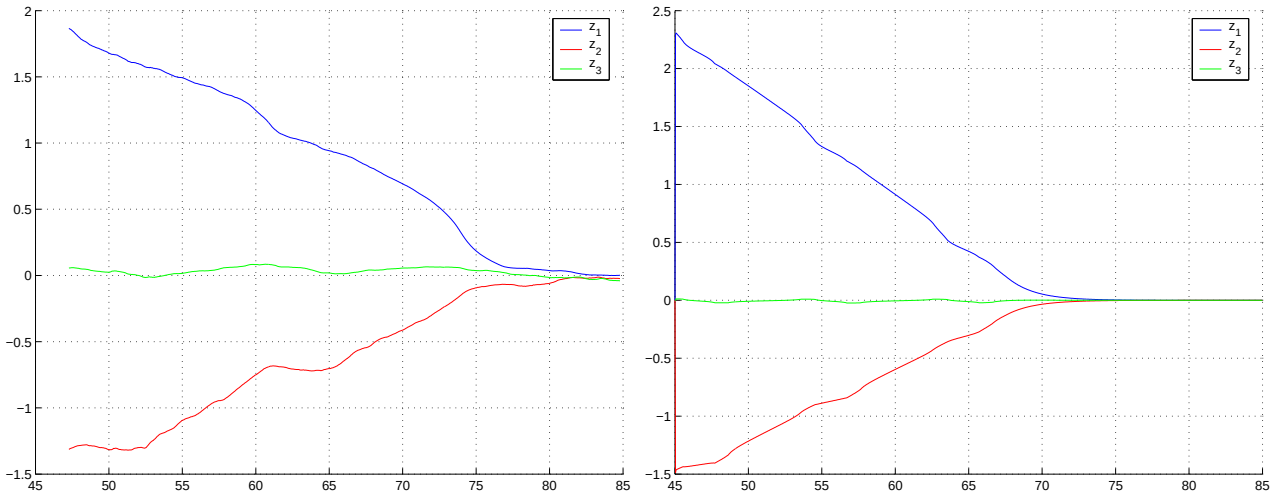

(a) State variables during experimentation (b) Simulation

Figure 7: State variables using estimated positions, $z = f(\theta)\hat{g}^{-1}$, with $\varepsilon_2 = 0.3$

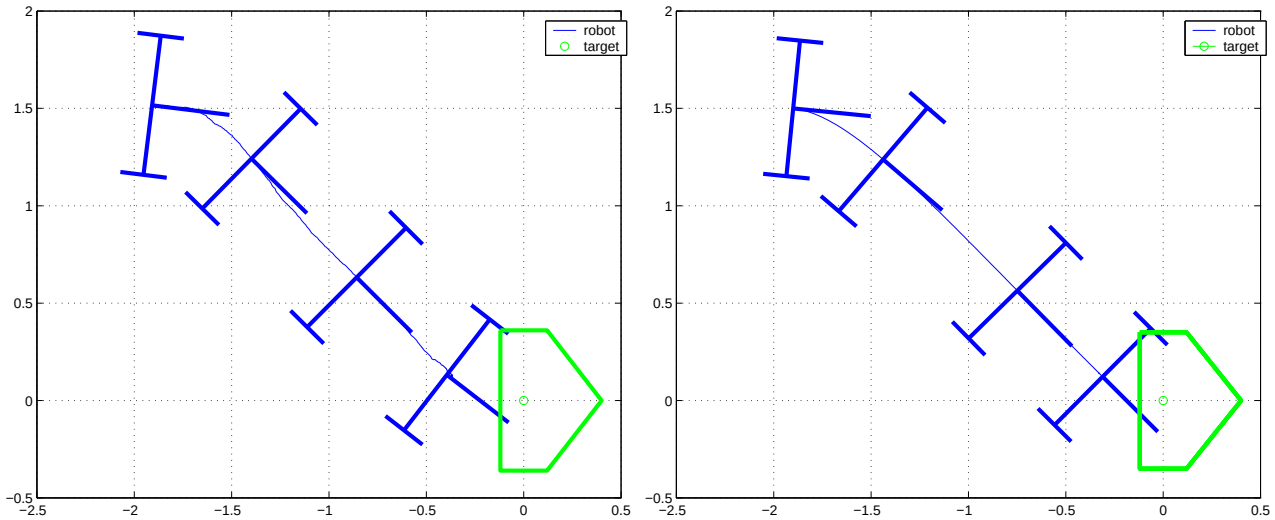

(a) Estimated trajectory during experimentation (b) Simulation

Figure 8: Cartesian motion of the robot $\varepsilon_2 = 1.0$

Conclusion

A new control strategy for the tracking of an omnidirectional target by a nonholonomic mobile robot has been experimented. Various issues related to the considered experimental setup (state variables and target velocity estimation from visual data and odometry, control discretization, input saturations...) have been addressed. A few other practical issues may deserve to be looked at more closely. For instance, visual data processing is responsible for delays in the measurement of the target's posture and this could be taken into account at the estimator's design level. It was also pointed out in Section 3 that using unprocessed measurements of the target/robot relative posture, by opposition to estimating this posture via a model of the target's motion, can sometimes be more accurate and can yield better results. This is especially true when the actual target's velocity varies significantly and rapidly (thus violating the considered model equation by large amount). This suggests working out some more on the estimator's design. Our plans for future studies also include an extension of the proposed control approach to car-like mobile robots, and its experimentation for the automatic tracking of a maneuvering car.

A Error system equations

By definition $\overrightarrow{\mathrm{P}_t\mathrm{P}_r} = x\vec{\imath}_t + y\vec{\jmath}_t$ Differentiating both sides of this equality with respect to time yields

$$\begin{aligned} \vec{\mathrm{V}}_{\mathrm{P}_r} - \vec{\mathrm{V}}_{\mathrm{P}_t} &= \dot{x}\vec{\imath}_t + x\tfrac{d}{dt}\vec{\imath}_t + \dot{y}\vec{\jmath}_t + y\tfrac{d}{dt}\vec{\jmath}_t \\ &= (\dot{x} - y\dot{\alpha}_t)\vec{\imath}_t + (\dot{y} + x\dot{\alpha}_t)\vec{\jmath}_t \end{aligned} \tag{28}$$

On the other hand, since $\alpha = \alpha_r - \alpha_t$, we have

$$\begin{aligned} \vec{\mathrm{V}}_{\mathrm{P}_r} &= u_1\vec{\imath}_r \\ &= u_1(\cos\alpha\vec{\imath}_t + \sin\alpha\vec{\jmath}_t) \end{aligned} \tag{29}$$

and from (2),

$$\vec{V}_{\mathrm{P}_t} = a\vec{\imath}_t + b\vec{\jmath}_t \tag{30}$$

By identifying (28) with (29) and (30), one obtains the two first equations of (4). The third one follows from (1) and (2).

B Transversality condition

The transversality condition is equivalent to the fact that the matrix

$$\begin{aligned} H(\theta) &\triangleq \begin{pmatrix} b_1(f(\theta)) & b_2 & -\dfrac{\partial f}{\partial\theta}(\theta) \end{pmatrix} \\ &= \begin{pmatrix} \cos(\varepsilon_2\cos\theta) & 0 & -\varepsilon_1\cos\theta \\ \sin(\varepsilon_2\cos\theta) & 0 & -\varepsilon_1\varepsilon_2\frac{\cos 2\theta}{2} \\ 0 & 1 & \varepsilon_2\sin\theta \end{pmatrix} \end{aligned}$$

is invertible for any θ. A simple calculation yields

$$\begin{aligned} \det H(\theta) &= \varepsilon_1\left(\varepsilon_2\frac{\cos 2\theta}{2}\cos(\varepsilon_2\cos\theta) - \sin(\varepsilon_2\cos\theta)\cos\theta\right) \\ &= \varepsilon_1\varepsilon_2\left(\frac{\cos 2\theta}{2}\cos(\varepsilon_2\cos\theta) - \frac{\sin(\varepsilon_2\cos\theta)}{\varepsilon_2\cos\theta}\cos^2\theta\right) \\ &= \varepsilon_1\varepsilon_2\left(\frac{\cos^2\theta - \sin^2\theta}{2}\cos(\varepsilon_2\cos\theta) - \frac{\sin(\varepsilon_2\cos\theta)}{\varepsilon_2\cos\theta}\cos^2\theta\right) \\ &= -\varepsilon_1\varepsilon_2\left[\cos^2\theta\left(\frac{\sin(\varepsilon_2\cos\theta)}{\varepsilon_2\cos\theta} - \frac{\cos(\varepsilon_2\cos\theta)}{2}\right) + \sin^2\theta\frac{\cos(\varepsilon_2\cos\theta)}{2}\right] \end{aligned}$$

For $\varepsilon_2 \in (0, \frac{\pi}{2}]$ and for any θ, we have

$$0 \le \frac{\cos(\varepsilon_2\cos\theta)}{2} \le \frac{1}{2}$$

and

$$0 < \frac{\sin(\varepsilon_2\cos\theta)}{\varepsilon_2\cos\theta} - \frac{\cos(\varepsilon_2\cos\theta)}{2}$$

One concludes that for $\varepsilon_1 > 0$ and $\varepsilon_2 \in (0, \frac{\pi}{2}]$,

$$\forall\theta, \qquad \det H(\theta) < 0 \tag{31}$$

so that f is a transverse function.

C Proofs of Section 3

C.1 Proof of Proposition 2

Let $\tilde{X}_p = X_p - \hat{X}_p$ and $\tilde{X}_\alpha = X_\alpha - \hat{X}_\alpha$. From (16), (17), and (19), we deduce that

$$\begin{aligned}\dot{\tilde{X}}_p &= A_p(\hat{c})\tilde{X}_p - D_p(p-\hat{p}) + U_p(\alpha) - U_p(\hat{\alpha}) + V_p - D_p v_p + (A_p(c) - A_p(\hat{c}))X_p \\ \dot{\tilde{X}}_\alpha &= A_\alpha \tilde{X}_\alpha - D_\alpha(\alpha - \hat{\alpha}) + V_\alpha - D_\alpha v_\alpha\end{aligned} \tag{32}$$

From (18),

$$p - \hat{p} = C_p \tilde{X}_p \quad \text{with} \quad C_p = \begin{pmatrix} 1 & 0 & 0 & 0 \\ 0 & 1 & 0 & 0 \end{pmatrix} \tag{33}$$

$$\alpha - \hat{\alpha} = C_\alpha \tilde{X}_\alpha \quad \text{with} \quad C_\alpha = (1\ 0) \tag{34}$$

and

$$A_p(c) - A_p(\hat{c}) = (c - \hat{c})A_1 = \tilde{X}_\alpha^T C_c A_1 \tag{35}$$

for some constant matrices C_c and A_1. Therefore, from (32), (33), (34), and (35),

$$\dot{\tilde{X}}_p = (A_p(\hat{c}) - D_p C_p)\tilde{X}_p + \tilde{X}_\alpha^T C_c A_1 X_p + U_p(\alpha) - U_p(\hat{\alpha}) + V_p - D_p v_p \tag{36a}$$

$$\dot{\tilde{X}}_\alpha = (A_\alpha - D_\alpha C_\alpha)\tilde{X}_\alpha + V_\alpha - D_\alpha v_\alpha \tag{36b}$$

Let us first consider System (36b). From (18), (20), and (34), one easily verifies that the matrix $A_\alpha - D_\alpha C_\alpha$ is Hurwitz-stable. Let $W_\alpha(X_\alpha)$ denote a quadratic positive definite Lyapunov function for the system

$$\dot{\tilde{X}}_\alpha = (A_\alpha - D_\alpha C_\alpha)\tilde{X}_\alpha$$

By definition of v_M, it follows from (18) that for some constant c_α,

$$\|V_\alpha - D_\alpha v_\alpha\| \leq c_\alpha v_M$$

Therefore, there exist positive constants γ and c'_α such that the derivative of $W_\alpha(X_\alpha)$ along the solutions of (36b) satisfies

$$\begin{aligned}\dot{W}_\alpha(\tilde{X}_\alpha) &\leq -\gamma W_\alpha(\tilde{X}_\alpha) + c_\alpha v_M \|\nabla W_\alpha(\tilde{X}_\alpha)\| \\ &\leq -\frac{\gamma}{2} W_\alpha(\tilde{X}_\alpha) + c'_\alpha v_M^2\end{aligned} \tag{37}$$

One deduces from this inequality that along any solution of (36b)

$$W_\alpha(\tilde{X}_\alpha(t)) \leq \frac{2}{\gamma} c'_\alpha v_M^2 + e^{-\frac{\gamma}{2}t} W_\alpha(\tilde{X}_\alpha(0)) \tag{38}$$

Since $W_\alpha(\tilde{X}_\alpha)$ is a quadratic definite positive function, it follows from (38) that for some positive constants d_α and d'_α,

$$\|\tilde{X}_\alpha(t)\| \leq d_\alpha v_M + d'_\alpha e^{-\frac{\gamma}{4}t} \|\tilde{X}_\alpha(0)\| \tag{39}$$

Since by assumption, u_1^o, u_2^o, and X_p are bounded, it follows from (18) and (39) that

$$\|\tilde{X}_\alpha^T C_c A_1 X_p + U_p(\alpha) - U_p(\hat{\alpha}) + V_p - D_p v_p\| \leq c_p v_M + c'_p e^{-\frac{\gamma}{4}t} \|\tilde{X}_\alpha(0)\| \tag{40}$$

The following technical Lemma is proved below

Lemma 2 *There exist a positive definite matrix P and a scalar $\tau > 0$ such that, for any function $\hat{c}(.)$, the derivative of $W_p \triangleq \frac{1}{2}\tilde{X}_p^T P \tilde{X}_p$ along the solutions of*

$$\dot{\tilde{X}}_p = (A_p(\hat{c}) - D_p C_p)\tilde{X}_p \tag{41}$$

satisfies

$$\dot{W}_p(\tilde{X}_p) \leq -\tau W_p(\tilde{X}_p) \tag{42}$$

By proceeding as for $\tilde{X}_\alpha$, one shows from (42) and (40) that for some positive constants d_p and d'_p, and along any solution to System (36a),

$$\|\tilde{X}_p(t)\| \leq d_p v_M + d'_p e^{-\frac{\gamma'}{4}t}\|\tilde{X}(0)\| \tag{43}$$

Proposition 2 follows from (39) and (43). There remains to prove Lemma 2.
Proof of Lemma 2: From (18) and (20),

$$A_p(\hat{c}) - D_p C_p = \begin{pmatrix} -\lambda_p & \hat{c} & -1 & 0 \\ -\hat{c} & -\lambda_p & 0 & -1 \\ \beta_p & 0 & 0 & \hat{c} \\ 0 & \beta_p & -\hat{c} & 0 \end{pmatrix}$$

We let

$$P = \begin{pmatrix} p_1 & 0 & p_3 & 0 \\ 0 & p_1 & 0 & p_3 \\ p_3 & 0 & p_2 & 0 \\ 0 & p_3 & 0 & p_2 \end{pmatrix} \tag{44}$$

where p_1, p_2, and p_3 will be specified later on. Then, the derivative of W_p along the solutions of (41) satisfies

$$\begin{aligned} \dot{W}_p(\tilde{X}_p) =& \tilde{x}_1^2(-p_1\lambda_p + p_3\beta_p) - \tilde{x}_3^2 p_3 + \tilde{x}_1\tilde{x}_3(p_2\beta_p - p_1 - p_3\lambda_p) \\ &+ \tilde{x}_2^2(-p_1\lambda_p + p_3\beta_p) - \tilde{x}_4^2 p_3 + \tilde{x}_2\tilde{x}_4(p_2\beta_p - p_1 - p_3\lambda_p) \end{aligned} \tag{45}$$

Let

$$p_1 \triangleq 2\beta_p,\ p_3 \triangleq \lambda_p,\ p_2 \triangleq \frac{p_1 + p_3\lambda_p}{\beta_p} = 2 + \frac{\lambda_p^2}{\beta_p} \tag{46}$$

Then, it follows from (45) that

$$\dot{W}(\tilde{X}_p) = -\lambda_p\beta_p(\tilde{x}_1^2 + \tilde{x}_2^2) - \lambda_p(\tilde{x}_3^2 + \tilde{x}_4^2)$$

so that $\dot{W}(\tilde{X}_p)$ is definite negative. There remains to show that W_p is positive definite. From (46),

$$\begin{aligned} \beta_p(p_1\tilde{x}_1^2 + p_2\tilde{x}_3^2 + 2p_3\tilde{x}_1\tilde{x}_3) &= 2\beta_p^2\tilde{x}_1^2 + (2\beta_p + \lambda_p^2)\tilde{x}_3^2 + 2\lambda_p\beta_p\tilde{x}_1\tilde{x}_3 \\ &\geq 2\beta_p^2\tilde{x}_1^2 + \lambda_p^2\tilde{x}_3^2 + 2\lambda_p\beta_p\tilde{x}_1\tilde{x}_3 \\ &\geq \beta_p^2\tilde{x}_1^2 + (\beta_p\tilde{x}_1 + \lambda_p\tilde{x}_3)^2 \end{aligned}$$

This implies that $p_1\tilde{x}_1^2 + p_2\tilde{x}_3^2 + 2p_3\tilde{x}_1\tilde{x}_3$ is a positive definite quadratic form in $\tilde{x}_1$ and $\tilde{x}_3$. Since, by (44),

$$W_p = (p_1\tilde{x}_1^2 + p_2\tilde{x}_3^2 + 2p_3\tilde{x}_1\tilde{x}_3) + (p_1\tilde{x}_2^2 + p_2\tilde{x}_4^2 + 2p_3\tilde{x}_2\tilde{x}_4)$$

the proof follows.

C.2 Proof of Lemma 1

C.2.1 α–estimator

The steady state optimal Kalman gain for the estimator (19b) is given (see e.g. [3, Sec. 4.4] for details) by $D_\alpha = \Sigma_\alpha C_\alpha^T \omega_\alpha^{-1}$, with $C_\alpha = (1,0)$ and Σ_α the positive definite solution of the algebraic Riccati equation associated with System (17b)–(16b):

$$0 = A_\alpha \Sigma_\alpha + \Sigma_\alpha A_\alpha^T - \Sigma_\alpha C_\alpha^T \omega_\alpha^{-1} C_\alpha \Sigma_\alpha + \left(\begin{smallmatrix} \omega_2 & 0 \\ 0 & \omega_c \end{smallmatrix}\right) \tag{47}$$

Since Σ_α is a covariance matrix, it is symmetric, so that we can write

$$\Sigma_\alpha = \begin{pmatrix} \Sigma_{11} & \Sigma_{12} \\ \Sigma_{12} & \Sigma_{22} \end{pmatrix} \tag{48}$$

Then, (47) is equivalent to

$$\left\{ \begin{array}{rcl} 2\Sigma_{12} + \frac{\Sigma_{11}^2}{\omega_\alpha} - \omega_2 & = & 0 \\ \Sigma_{22} + \frac{\Sigma_{11}\Sigma_{12}}{\omega_\alpha} & = & 0 \\ \frac{\Sigma_{12}^2}{\omega_\alpha} - \omega_c & = & 0 \end{array} \right. \tag{49}$$

Using the fact that Σ_α must be positive definite, and the assumption $\omega_2 \ll \sqrt{\omega_c \omega_\alpha}$, one obtains the following solution to (49):

$$\left\{ \begin{array}{rcl} \Sigma_{11} & = & \sqrt{\omega_\alpha(\omega_2 + 2\sqrt{\omega_c\omega_\alpha})} \\ \Sigma_{12} & = & -\sqrt{\omega_c\omega_\alpha} \\ \Sigma_{22} & = & \sqrt{\omega_c(\omega_2 + 2\sqrt{\omega_c\omega_\alpha})} \end{array} \right. \tag{50}$$

From (48), (50), and the definition of D_α, we finally obtain

$$D_\alpha = \begin{pmatrix} \sqrt{\frac{\omega_2}{\omega_\alpha} + 2\sqrt{\frac{\omega_c}{\omega_\alpha}}} \\ -\sqrt{\frac{\omega_c}{\omega_\alpha}} \end{pmatrix} \tag{51}$$

Under the assumption that $\omega_2 \ll \sqrt{\omega_c\omega_\alpha}$, D_α can therefore be approximated by

$$D_\alpha \approx \begin{pmatrix} \sqrt{2}\lambda_\alpha \\ -\lambda_\alpha^2 \end{pmatrix} \quad \lambda_\alpha = \sqrt[4]{\frac{\omega_c}{\omega_\alpha}} \tag{52}$$

and (21) follows.

C.2.2 p–estimator

We consider the steady state optimal Kalman gain D_p for the estimator (19a) associated with System (17a)–(16a). Under the assumption that c is constant and that $\omega_1 \equiv 0$, D_p is given by $D_p = \Sigma_p C_p^T \omega_p^{-1}$, with $C_p = (\mathrm{I}_2, 0_2)$ and Σ_p the positive definite solution of the algebraic Riccati equation associated with System (17a)–(16a):

$$0 = A_p \Sigma_p + \Sigma_p A_p^T - \Sigma_p C_p^T \omega_p^{-1} C_p \Sigma_p + V \tag{53}$$

with

$$V = \begin{pmatrix} 0 & 0 & 0 & 0 \\ 0 & 0 & 0 & 0 \\ 0 & 0 & \omega_a & 0 \\ 0 & 0 & 0 & \omega_b \end{pmatrix} \quad \omega_p = \begin{pmatrix} \omega_x & 0 \\ 0 & \omega_y \end{pmatrix}$$

Let us first consider the case $c = 0$. Then

$$A_p(\hat{c}) = A_p = \begin{pmatrix} 0 & 0 & -1 & 0 \\ 0 & 0 & 0 & -1 \\ 0 & 0 & 0 & 0 \\ 0 & 0 & 0 & 0 \end{pmatrix}$$

and the systems (17a) and (16a) define two decoupled systems similar to the systems (17b) and (16b) when ω_2 is neglected:

$$\left\{ \begin{array}{rcl} \begin{pmatrix} \dot{x} \\ \dot{a} \end{pmatrix} & = & A_\alpha \begin{pmatrix} x \\ a \end{pmatrix} + \begin{pmatrix} u_1^o \cos\alpha \\ 0 \end{pmatrix} + \begin{pmatrix} 0 \\ v_a \end{pmatrix} \\ x^v & = & x + v_x \end{array} \right. \tag{54a}$$

$$\left\{ \begin{array}{rcl} \begin{pmatrix} \dot{y} \\ \dot{b} \end{pmatrix} & = & A_\alpha \begin{pmatrix} y \\ b \end{pmatrix} + \begin{pmatrix} u_1^o \sin\alpha \\ 0 \end{pmatrix} + \begin{pmatrix} 0 \\ v_b \end{pmatrix} \\ y^v & = & y + v_y \end{array} \right. \tag{54b}$$

By using the previous results in Appendix C.2.1 for the α–estimator, we obtain the following steady state Kalman gain D_p for Systems (17a) and (16a):

$$D_p \approx \begin{pmatrix} \sqrt{2}\lambda_1 & 0 \\ 0 & \sqrt{2}\lambda_2 \\ -\lambda_1^2 & 0 \\ 0 & -\lambda_2^2 \end{pmatrix} \quad \lambda_1 = \sqrt[4]{\frac{\omega_a}{\omega_x}} \quad \lambda_2 = \sqrt[4]{\frac{\omega_b}{\omega_y}} \tag{55}$$

Similarly, from (48) and (50) one deduces the steady state covariance matrix Σ_p

$$\Sigma_p = \begin{pmatrix} \sqrt{2\omega_x\sqrt{\omega_a\omega_x}} & 0 & -\sqrt{\omega_a\omega_x} & 0 \\ 0 & \sqrt{2\omega_y\sqrt{\omega_b\omega_y}} & 0 & -\sqrt{\omega_b\omega_y} \\ -\sqrt{\omega_a\omega_x} & 0 & \sqrt{2\omega_a\sqrt{\omega_a\omega_x}} & 0 \\ 0 & -\sqrt{\omega_b\omega_y} & 0 & \sqrt{2\omega_b\sqrt{\omega_b\omega_y}} \end{pmatrix} \tag{56}$$

Let us now consider the case $c \neq 0$. We show below, under the assumption that $\omega_a = \omega_b$ and $\omega_x = \omega_y$, that Σ_p defined by (56) is also the positive definite solution to the algebraic Riccati equation associated with System (17a)–(16a), so that D_p defined by (55) is also the steady state Kalman gain for the p-estimator (19a).

From the definition (18) of $A_p(\hat{c})$, (53) is equivalent to

$$\begin{pmatrix} c\mathrm{J}_2 & -\mathrm{I}_2 \\ 0_2 & c\mathrm{J}_2 \end{pmatrix} \Sigma_p + \Sigma_p \begin{pmatrix} -c\mathrm{J}_2 & 0_2 \\ -\mathrm{I}_2 & -c\mathrm{J}_2 \end{pmatrix} - \Sigma_p \begin{pmatrix} \mathrm{I}_2 \\ 0_2 \end{pmatrix} \omega_p^{-1} \begin{pmatrix} \mathrm{I}_2 & 0_2 \end{pmatrix} \Sigma_p + V = 0 \tag{57}$$

with $\mathrm{J}_2 = \left(\begin{smallmatrix} 0 & 1 \\ -1 & 0 \end{smallmatrix}\right)$. Let us decompose Σ_p as

$$\Sigma_p = \begin{pmatrix} \Sigma_{11} & \Sigma_{12} \\ \Sigma_{12}^T & \Sigma_{22} \end{pmatrix} \tag{58}$$

where each Σ_{ij} is a 2×2 matrix. Then (57) is equivalent to

$$\left\{ \begin{array}{rcl} c(\mathrm{J}_2\Sigma_{11} - \Sigma_{11}\mathrm{J}_2) - (\Sigma_{12} + \Sigma_{12}^T) - \Sigma_{11}{\omega_p}^{-1}\Sigma_{11} & = & 0 \\ c(\mathrm{J}_2\Sigma_{12} - \Sigma_{12}\mathrm{J}_2) - \Sigma_{22} - \Sigma_{11}{\omega_p}^{-1}\Sigma_{12} & = & 0 \\ c(\mathrm{J}_2\Sigma_{22} - \Sigma_{22}\mathrm{J}_2) - \Sigma_{12}^T{\omega_p}^{-1}\Sigma_{12} + \left(\begin{smallmatrix} \omega_a & 0 \\ 0 & \omega_b \end{smallmatrix}\right) & = & 0 \end{array} \right. \tag{59}$$

If we identify Σ_p, as given by (56), with the general expression (58), then (59) becomes:

$$\left\{\begin{array}{rcl} c\begin{pmatrix} 0 & \sqrt{2\omega_y\sqrt{\omega_b\omega_y}}-\sqrt{2\omega_x\sqrt{\omega_a\omega_x}} \\ \sqrt{2\omega_y\sqrt{\omega_b\omega_y}}-\sqrt{2\omega_x\sqrt{\omega_a\omega_x}} & 0 \end{pmatrix} & = & 0 \\ c\begin{pmatrix} 0 & \sqrt{\omega_a\omega_x}-\sqrt{\omega_b\omega_y} \\ \sqrt{\omega_a\omega_x}-\sqrt{\omega_b\omega_y} & 0 \end{pmatrix} & = & 0 \\ c\begin{pmatrix} 0 & \sqrt{2\omega_b\sqrt{\omega_b\omega_y}}-\sqrt{2\omega_a\sqrt{\omega_a\omega_x}} \\ \sqrt{2\omega_b\sqrt{\omega_b\omega_y}}-\sqrt{2\omega_a\sqrt{\omega_a\omega_x}} & 0 \end{pmatrix} & = & 0 \end{array}\right. \tag{60}$$

Therefore, if $\omega_a = \omega_b$ and $\omega_x = \omega_y$, Equation (60) is satisfied and the proof follows.

D Proof of Proposition 3

Preliminary remark: In this section many inequalities of the type $\|X\| \leq c_1 v_M^{p_1} + \ldots + c_k v_M^{p_k}$ are involved, for some positive c_i's and some integers $0 \leq p_1 < p_2 \ldots < p_k$. Since Proposition 3 only concerns "small enough" values of v_M, such inequalities can be simplified as $\|X\| \leq c v_M^{p_1}$. Such simplifications will be done repeatedly, without further notice.

From the definition of z in Proposition 1, it can be shown — see also [4] — that

$$\dot{z} = -dr_{g^{-1}}(f)\left(H(\theta)\bar{u} + dl_z(g)b_0(g,u_t)\right) \tag{61}$$

From (12), the feedback law $\bar{u}(g^e, \hat{u}_t, \theta)$ is given by

$$\bar{u}(g^e,\hat{u}_t,\theta) = -H(\theta)^{-1}\left(dl_{z^e}(g^e)b_0(g^e,\hat{u}_t) + dr_{g^e}(z^e)Kz^e\right) \tag{62}$$

with $z^e \triangleq f(\theta)(g^e)^{-1}$. Therefore, applying this feedback law to System (61) yields

$$\begin{aligned} \dot{z} &= dr_{g^{-1}}(f)dr_{g^e}(z^e)Kz^e - dr_{g^{-1}}(f)(dl_z(g)b_0(g,u_t) - dl_{z^e}(g^e)b_0(g^e,\hat{u}_t) \\ &= Kz^e + \Gamma_1 Kz^e - \Gamma_2 \\ &= Kz - K(z-z^e) + \Gamma_1 Kz^e - \Gamma_2 \end{aligned} \tag{63}$$

with

$$\Gamma_1 \triangleq dr_{g^{-1}}(f)dr_{g^e}(z^e) - I\,, \quad \Gamma_2 \triangleq dr_{g^{-1}}(f)\left(dl_z(g)b_0(g,u_t) - dl_{z^e}(g^e)b_0(g^e,\hat{u}_t)\right) \tag{64}$$

From (11), it follows that if $g_1 = (p_1, \alpha_1)$ and $g_2 = (p_2, \alpha_2)$,

$$dr_{g_2}(g_1) = \begin{pmatrix} I & SR(\alpha_1)p_2 \\ 0 & 1 \end{pmatrix}, \quad dl_{g_1}(g_2) = \begin{pmatrix} R(\alpha_1) & 0 \\ 0 & 1 \end{pmatrix}, \quad g_1^{-1} = \begin{pmatrix} -R(-\alpha_1)p_1 \\ -\alpha_1 \end{pmatrix} \tag{65}$$

with

$$S = \begin{pmatrix} 0 & -1 \\ 1 & 0 \end{pmatrix}$$

Therefore, using (64), (65), and the fact that the orientation component z_α of z is given by $z_\alpha = f_\alpha - \alpha$, we obtain that

$$\Gamma_1 = \begin{pmatrix} 0 & \Gamma_{1,p} \\ 0 & 0 \end{pmatrix} \quad \text{with } \Gamma_{1,p} \triangleq S\big(R(z_\alpha^e)p^e - R(z_\alpha)p\big) \tag{66}$$

Let us now consider the term Γ_2 in (64). From (6) and (65), one shows that

$$dl_z(g)b_0(g,u_t) - dl_{z^e}(g^e)b_0(g^e,\hat{u}_t) = \begin{pmatrix} \hat{c}R(z_\alpha^e)Sp^e - cR(z_\alpha)Sp + R(z_\alpha^e)(\hat{a},\hat{b})^T - R(z_\alpha)(a,b)^T \\ -\tilde{c} \end{pmatrix}$$

so that, by using (65) again, it follows from (64) that

$$\Gamma_2 = \begin{pmatrix} \Gamma_{2,p} \\ \Gamma_{2,\alpha} \end{pmatrix} = \begin{pmatrix} \hat{c}R(z_\alpha^e)Sp^e - cR(z_\alpha)Sp + R(z_\alpha^e)(\hat{a},\hat{b})^T - R(z_\alpha)(a,b)^T + \tilde{c}SR(z_\alpha)p \\ -\tilde{c} \end{pmatrix} \tag{67}$$

From (23), (66), and (67), we can rewrite (63) as follows:

$$\left\{ \begin{array}{ll} \dot{z}_p & = K_p z_p - K_p(z_p - z_p^e) + \Gamma_{1,p} k_\alpha z_\alpha^e - \Gamma_{2,p} \\ \dot{z}_\alpha & = k_\alpha z_\alpha - k_\alpha(z_\alpha - z_\alpha^e) + \tilde{c} \end{array} \right. \tag{68}$$

with z_p and z_α the position and orientation component of z, i.e. $z^T = (z_p^T, z_\alpha)$.

From (68) and Equation (36) which gives the estimation error dynamics, we obtain :

$$\left\{ \begin{array}{ll} \dot{z}_p & = K_p z_p - K_p(z_p - z_p^e) + \Gamma_{1,p} k_\alpha z_\alpha^e - \Gamma_{2,p} \\ \dot{\tilde{X}}_p & = (A_p(\hat{c}) - D_p C_p)\tilde{X}_p + \tilde{X}_\alpha^T C_c A_1 X_p + U_p(\alpha) - U_p(\hat{\alpha}) + V_p - D_p v_p \end{array} \right. \tag{69}$$

and

$$\left\{ \begin{array}{ll} \dot{z}_\alpha & = k_\alpha z_\alpha - k_\alpha(z_\alpha - z_\alpha^e) + \tilde{c} \\ \dot{\tilde{X}}_\alpha & = (A_\alpha - D_\alpha C_\alpha)\tilde{X}_\alpha + V_\alpha - D_\alpha v_\alpha \end{array} \right. \tag{70}$$

We first consider System (70). Since $z = f(\theta)g^{-1}$ and $z^e = f(\theta)(g^e)^{-1}$, it follows from (11) and (65) that $z_\alpha - z_\alpha^e = f_\alpha - \alpha - (f_\alpha - \alpha^e) = \alpha^e - \alpha$. Therefore, we can rewrite (70) as

$$\left\{ \begin{array}{ll} \dot{z}_\alpha & = k_\alpha z_\alpha - k_\alpha(\alpha^e - \alpha) + \tilde{c} \\ \dot{\tilde{X}}_\alpha & = (A_\alpha - D_\alpha C_\alpha)\tilde{X}_\alpha + V_\alpha - D_\alpha v_\alpha \end{array} \right. \tag{71}$$

Let us consider the two possible choices for g^e considered in Proposition 3. First, if $g^e = \hat{g}$, then, $\alpha^e - \alpha = \hat{\alpha} - \alpha = -\tilde{\alpha}$. In this case, System (71) is the equation of an asymptotically stable linear system — this can be checked directly and also follows from the separation principle in linear system theory —, perturbed by the term $(0, V_\alpha - D_\alpha v_\alpha)^T$. Since this term is bounded in norm by $c\, v_M$ for some constant c, it follows that there exists a quadratic Lyapunov function $L_\alpha(z_\alpha, \tilde{X}_\alpha)$ such that, along the trajectories of (71),

$$\dot{L}_\alpha \leq -2\tau_\alpha L_\alpha + c_\alpha v_M^2 \quad (\tau_\alpha > 0) \tag{72}$$

If g^e is such that $\|g^e - g\| \leq \gamma v_M$, then $|\alpha^e - \alpha| \leq \gamma v_M$. In this case, System (71) is still the equation of an asymptotically stable linear system, perturbed by the term $(-k_\alpha(\alpha^e - \alpha), V_\alpha - D_\alpha v_\alpha)^T$. Since this term is also bounded in norm by $c\, v_M$ for some constant c, (72) holds again — for some possibly different quadratic Lyapunov function L_α.

We now consider System (69). One can rewrite this system as

$$\left\{ \begin{array}{ll} \dot{z}_p & = K_p z_p - \Delta_1 \\ \dot{\tilde{X}}_p & = (A_p(\hat{c}) - D_p C_p)\tilde{X}_p + \Delta_2 \end{array} \right. \tag{73}$$

with

$$\left\{ \begin{array}{l} \Delta_1 \triangleq K_p(z_p - z_p^e) - \Gamma_{1,p} k_\alpha z_\alpha^e + \Gamma_{2,p} \\ \Delta_2 \triangleq \tilde{X}_\alpha^T C_c A_1 X_p + U_p(\alpha) - U_p(\hat{\alpha}) + V_p - D_p v_p \end{array} \right. \tag{74}$$

The proof of the following technical lemma is given at the end of this section.

Lemma 3 *There exists a constant c such that*

$$\left\{ \begin{array}{l} \|\Delta_1\| \leq c(1 + \|z_p\|)(v_M + \sqrt{L_\alpha} + L_\alpha) + c\|\tilde{X}_p\|(1 + \sqrt{L_\alpha}) \\ \|\Delta_2\| \leq c(1 + \|z_p\| + \|\tilde{X}_p\|)(v_M + \sqrt{L_\alpha} + L_\alpha) \end{array} \right. \tag{75}$$

Let Q denote a symmetric positive definite matrix such that

$$QK_p + K_p^T Q \leq -2\gamma_o I \qquad (\gamma_o > 0) \tag{76}$$

Such a matrix exists because K is Hurwitz stable so that, by (23), K_p is also Hurwitz stable. Consider the function

$$L_p(z_p, \tilde{X}_p) = z_p^T Q z_p + \beta W(\tilde{X}_p) \tag{77}$$

with β a positive parameter which will be specified further, and W the Lyapunov function in Lemma 2. By differentiating L_p along the trajectories of (73), we obtain:

$$\dot{L}_p = \frac{\partial L_p}{\partial z_p} K_p z_p + \frac{\partial L_p}{\partial \tilde{X}_p}(A_p(\hat{c}) - K_p C_p)\tilde{X}_p - \frac{\partial L_p}{\partial z_p}\Delta_1 + \frac{\partial L_p}{\partial \tilde{X}_p}\Delta_2 \tag{78}$$

From (42) and (76) and the fact that Q is positive definite, we deduce from (78) that

$$\dot{L}_p \leq -3\gamma\|z_p\|^2 - 3\beta\gamma'\|\tilde{X}_p\|^2 + \|\frac{\partial L_p}{\partial z_p}\|\|\Delta_1\| + \|\frac{\partial L}{\partial \tilde{X}_p}\|\|\Delta_2\| \tag{79}$$

for some $\gamma, \gamma' > 0$. It follows from (75) and (77) that for some constant c,

$$\|\frac{\partial L_p}{\partial \tilde{X}_p}\|\|\Delta_2\| = \beta\|\frac{\partial W}{\partial \tilde{X}_p}\|\|\Delta_2\| \leq \beta c\|\tilde{X}_p\|\|\Delta_2\| \leq \beta\gamma'\|\tilde{X}_p\|\frac{c}{\gamma'}\|\Delta_2\| \leq \frac{\beta\gamma'}{2}\|\tilde{X}_p\|^2 + \frac{\beta c^2}{2\gamma'}\|\Delta_2\|^2 \tag{80}$$

By similar arguments, we show that for some other constant, again denoted as c,

$$\|\frac{\partial L_p}{\partial z_p}\|\|\Delta_1\| \leq \frac{\gamma}{2}\|z_p\|^2 + \frac{c^2}{2\gamma}\|\Delta_1\|^2 \tag{81}$$

From (79), (80), and (81), we get

$$\dot{L}_p \leq -2\gamma\|z_p\|^2 - 2\beta\gamma'\|\tilde{X}_p\|^2 + \frac{c^2}{2\gamma}\|\Delta_1\|^2 + \frac{\beta c^2}{2\gamma'}\|\Delta_2\|^2 \tag{82}$$

We deduce from (75) and (82) that for some constant c,

$$\begin{aligned}
\dot{L}_p \leq\ & -2\gamma\|z_p\|^2 - 2\beta\gamma'\|\tilde{X}_p\|^2 + c(1+\|z_p\|^2)(v_M^2 + L_\alpha + L_\alpha^2) \\
& + c(1+L_\alpha)\|\tilde{X}_p\|^2 + \beta c(1+\|z_p\|^2+\|\tilde{X}_p\|^2)(v_M^2 + L_\alpha + L_\alpha^2) \\
\leq\ & -\|z_p\|^2\left(2\gamma - c(1+\beta)(v_M^2 + L_\alpha + L_\alpha^2)\right) \\
& -\|\tilde{X}_p\|^2\left(2\beta\gamma' - c(1+L_\alpha) - \beta c(v_M^2 + L_\alpha + L_\alpha^2)\right) + c(1+\beta)(v_M^2 + L_\alpha + L_\alpha^2)
\end{aligned} \tag{83}$$

Let us first show the stability, for $v_M = 0$, of the controller/observer. For $v_M = 0$, we deduce from (72) and (83) that

$$\dot{L}_\alpha \leq -2\tau_\alpha L_\alpha \tag{84a}$$

$$\begin{aligned}
\dot{L}_p \leq & -\|z_p\|^2(2\gamma - c(1+\beta)(L_\alpha + L_\alpha^2) - \|\tilde{X}_p\|^2(2\beta\gamma' - c(1+L_\alpha) - \beta c(L_\alpha + L_\alpha^2)) \\
& + c(1+\beta)(L_\alpha + L_\alpha^2)
\end{aligned} \tag{84b}$$

Therefore, for any $\beta > 0$ such that $\beta\gamma' > c$, there exists $l_m > 0$ such that, for $L_\alpha \leq l_m$,

$$\dot{L}_p \leq -\tau_p L_p + \beta c(L_\alpha + L_\alpha^2) \quad (\tau_p > 0) \tag{85}$$

The stability of the closed-loop system follows from (84a) and (85). Let us now prove that $\|z\| + \|\tilde{X}\|$ is ultimately bounded by a value proportional to v_M, when v_M is small enough. Consider any $\beta > 0$ satisfying $\beta\gamma' > 2c$. Then, there exists some $\bar{v} > 0$ such that for any $v_M \in [0, \bar{v}]$,

$$\left\{ \begin{array}{rl} \gamma \geq & c(1+\beta)((1+\frac{c_\alpha}{\tau_\alpha})v_M^2 + \frac{c_\alpha^2}{\tau_\alpha^2}v_M^4) \\ \beta\gamma' \geq & c(1+\frac{c_\alpha}{\tau_\alpha}v_M^2) + \beta c((1+\frac{c_\alpha}{\tau_\alpha})v_M^2 + \frac{c_\alpha^2}{\tau_\alpha^2}v_M^4) \end{array} \right. \tag{86}$$

where c_α and τ_α are defined by (72). From (72), one easily shows that, along any trajectory of the closed-loop system,

$$L_\alpha(t) \leq L_\alpha(0)e^{-2\tau_\alpha t} + \frac{c_\alpha}{2\tau_\alpha}v_M^2$$

so that there exists a time instant T such that,

$$t \geq T \Longrightarrow L_\alpha(t) \leq \frac{c_\alpha}{\tau_\alpha}v_M^2 \tag{87}$$

We deduce from (83) and (87) that

$$\begin{array}{rl} \dot{L}_p \leq & -\|z_p\|^2\left(2\gamma - c(1+\beta)((1+\frac{c_\alpha}{\tau_\alpha})v_M^2 + \frac{c_\alpha^2}{\tau_\alpha^2}v_M^4)\right) \\ & -\|\tilde{X}_p\|^2\left(2\beta\gamma' - c(1+\frac{c_\alpha}{\tau_\alpha}v_M^2) - \beta c((1+\frac{c_\alpha}{\tau_\alpha})v_M^2 + \frac{c_\alpha^2}{\tau_\alpha^2}v_M^4)\right) \\ & +\beta c((1+\frac{c_\alpha}{\tau_\alpha})v_M^2 + \frac{c_\alpha^2}{\tau_\alpha^2}v_M^4) \end{array} \tag{88}$$

From (86) and (88),

$$\begin{array}{rll} t \geq T \Longrightarrow \dot{L}_p & \leq -\gamma\|z_p\|^2 - \beta\gamma'\|\tilde{X}_p\|^2 + \beta c((1+\frac{c_\alpha}{\tau_\alpha})v_M^2 + \frac{c_\alpha^2}{\tau_\alpha^2}v_M^4) \\ & \leq -2\tau_p L_p + c_p v_M^2 \end{array} \tag{89}$$

for some $\tau_p, c_p > 0$. The ultimate boundedness of $\|z\| + \|\tilde{X}\|$ by a value proportional to v_M, follows from (87) and (89) by using the fact that both L_α and L_p are quadratic functions.

Proof of Lemma 3: From (11),

$$z = \begin{pmatrix} z_p \\ z_\alpha \end{pmatrix} = \begin{pmatrix} f_p - R(z_\alpha)p \\ f_\alpha - \alpha \end{pmatrix} \tag{90}$$

Therefore, $p = R(-z_\alpha)(f_p - z_p)$, and since f is a bounded function

$$\|p\| \leq c(1 + \|z_p\|) \tag{91}$$

for some constant c. It also follows from (90) that

$$z - z^e = \begin{pmatrix} z_p - z_p^e \\ z_\alpha - z_\alpha^e \end{pmatrix} = \begin{pmatrix} R(z_\alpha^e)p^e - R(z_\alpha)p \\ \alpha^e - \alpha \end{pmatrix} = \begin{pmatrix} R(z_\alpha^e)(-(p-p^e) + (I - R(\alpha^e - \alpha))p) \\ \alpha^e - \alpha \end{pmatrix} \tag{92}$$

For both choices of g^e, i.e. $g^e = \hat{g}$ and $\|g^e - g\| \leq \gamma v_M$, we remark that

$$|\alpha - \alpha^e| \leq \gamma v_M + |\tilde{\alpha}| \leq c(v_M + \sqrt{L_\alpha}) \quad \text{and} \quad \|p - p^e\| \leq \gamma v_M + \|\tilde{p}\| \leq \gamma v_M + \|\tilde{X}_p\| \tag{93}$$

From (91), (92), and (93),

$$\begin{array}{rl} \|z_p - z_p^e\| & \leq \|p - p^e\| + c|\alpha^e - \alpha|(1 + \|z_p\|) \\ & \leq c(v_M + \sqrt{L_\alpha})(1 + \|z_p\|) + \|\tilde{X}_p\| \end{array} \tag{94}$$

Let us now consider the term $\Gamma_{1,p} k_\alpha z_\alpha^e$ in (74). We deduce from (66) and (92) that $\Gamma_{1,p} = S(z_p - z_p^e)$. This implies that $\|\Gamma_{1,p}\|$ satisfies the same inequality as $\|z_p - z_p^e\|$ in (94). From (90), (92), and (93), we also have

$$|z_\alpha^e| = |z_\alpha + (\alpha - \alpha^e)| \leq |z_\alpha| + |\alpha - \alpha^e| \leq c(v_M + \sqrt{L_\alpha}) \tag{95}$$

from which we finally deduce that

$$\|\Gamma_{1,p} k_\alpha z_\alpha^e\| \leq c(v_M^2 + L_\alpha)(1 + \|z_p\|) + c(v_M + \sqrt{L_\alpha})\|\tilde{X}_p\| \tag{96}$$

Let us finally consider the term $\Gamma_{2,p}$ in (74). From (67),

$$\begin{aligned} \Gamma_{2,p} =& (\tilde{c} - c) R(z_\alpha^e) S(p - p^e) + \left(\tilde{c} S R(z_\alpha) - \tilde{c} R(z_\alpha^e) S + c R(z_\alpha^e)(I - R(\alpha^e - \alpha)) S \right) p \\ & - R(z_\alpha^e)(\tilde{a}, \tilde{b})^T + R(z_\alpha^e)(I - R(\alpha^e - \alpha))(a, b)^T \end{aligned} \tag{97}$$

From (97) and (91), there exists a constant δ such that

$$\|\Gamma_{2,p}\| \leq \delta \|p - p^e\|(|\tilde{c}| + \|u_t\|) + \delta(|\tilde{c}| + \|u_t\||\alpha^e - \alpha|)(1 + \|z_p\|) + \|(\tilde{a}, \tilde{b})\| + \delta|\alpha^e - \alpha|\|u_t\| \tag{98}$$

We deduce from (93), (98), and the assumption that u_t is bounded that

$$\|\Gamma_{2,p}\| \leq \delta(v_M + \|\tilde{X}_p\|) \left(1 + \sqrt{L_\alpha}\right) + c \left(v_M + \sqrt{L_\alpha}\right) (1 + \|z_p\|) \tag{99}$$

The first inequality in (75) follows from (94), (96), and (99).

Let us now show the second inequality in (75). From (91) and the assumption that u_t is bounded,

$$\|\tilde{X}_\alpha^T C_c A_1 X_p\| \leq c(1 + \|z_p\|)\sqrt{L_\alpha} \tag{100}$$

It also follows from (18) that

$$\|V_p - D_p v_p\| \leq c v_M \tag{101}$$

There remains to consider the term $U_p(\alpha) - U_p(\hat{\alpha})$ in (74). We first derive an upperbound of $\|\bar{u}\|$, with $\bar{u}$ denoting the feedback law defined by (62). From (6) and (65),

$$\begin{aligned} dl_{z^e}(g^e) b_0(g^e, \hat{u}_t) &= \begin{pmatrix} R(z_\alpha^e) & 0 \\ 0 & 1 \end{pmatrix} \begin{pmatrix} -\hat{c} S p^e - \begin{pmatrix} \hat{a} \\ \hat{b} \end{pmatrix} \\ -\hat{c} \end{pmatrix} = \begin{pmatrix} -\hat{c} R(z_\alpha^e) S p^e - R(z_\alpha^e) \begin{pmatrix} \hat{a} \\ \hat{b} \end{pmatrix} \\ -\hat{c} \end{pmatrix} \\ &= \begin{pmatrix} -c R(z_\alpha^e) S p^e - R(z_\alpha^e) \begin{pmatrix} a \\ b \end{pmatrix} \\ -c \end{pmatrix} + \begin{pmatrix} \tilde{c} R(z_\alpha^e) S p^e + R(z_\alpha^e) \begin{pmatrix} \tilde{a} \\ \tilde{b} \end{pmatrix} \\ \tilde{c} \end{pmatrix} \end{aligned}$$

From these equalities and the boundedness assumption on u_t,

$$\|dl_{z^e}(g^e) b_0(g^e, \hat{u}_t)\| \leq k(1 + \|p^e\|)(1 + \|\tilde{c}\|) + \|(\tilde{a}, \tilde{b})\| \tag{102}$$

for some constant k. From (91) and (93),

$$\|p^e\| \leq k(1 + \|z_p\| + \|\tilde{X}_p\|) \tag{103}$$

and we deduce from (102) that

$$\|dl_{z^e}(g^e) b_0(g^e, \hat{u}_t)\| \leq k(1 + \|z_p\| + \|\tilde{X}_p\|)(1 + \sqrt{L_\alpha}) \tag{104}$$

From (23) and (65),

$$dr_{g^e}(z^e) K z^e = \begin{pmatrix} I & S R(z_\alpha^e) p^e \\ 0 & 1 \end{pmatrix} \begin{pmatrix} K_p z_p^e \\ k_\alpha z_\alpha^e \end{pmatrix} = \begin{pmatrix} K_p z_p^e + k_\alpha z_\alpha^e S R(z_\alpha^e) p^e \\ k_\alpha z_\alpha^e \end{pmatrix}$$

so that

$$\begin{aligned}\|dr_{g^e}(z^e)Kz^e\| &\leq k(|z^e_\alpha| + \|z^e_p\| + |z^e_\alpha|\|p^e\|)\\ &\leq k(|z^e_\alpha| + 1 + \|p^e\| + |z^e_\alpha|\|p^e\|)\\ &\leq k(1+\|p^e\|)(1+|z^e_\alpha|)\\ &\leq k(1+\|z_p\| + \|\tilde{X}_p\|)(1+\sqrt{L_\alpha})\end{aligned} \tag{105}$$

where the second inequality comes from (90), and the fourth from (95) and (103). From (62), (104), and (105),

$$\|\bar{u}\| \leq k(1+\|z_p\| + \|\tilde{X}_p\|)(1+\sqrt{L_\alpha}) \tag{106}$$

From (18),

$$\|U_p(\alpha) - U_p(\hat{\alpha})\| \leq |\alpha - \hat{\alpha}|\|u^o\| \leq |\tilde{\alpha}|(\|\bar{u}\| + 2v_M) \tag{107}$$

We finally obtain from (106) and (107) that

$$\|U_p(\alpha) - U_p(\hat{\alpha})\| \leq k\sqrt{L_\alpha}(1+\|z_p\| + \|\tilde{X}_p\|)(1+\sqrt{L_\alpha}) \tag{108}$$

The second inequality in (75) follows from (100), (101), and (108).

E Calculation details for the control implementation

E.1 Control discretization

E.1.1 α–estimator

The estimator (19b) is implemented in discrete form via a two steps prediction/correction procedure:

1. Integration over $[kT, (k+1)T)$ of the equation

$$\dot{\hat{X}}^-_\alpha = A_\alpha \hat{X}^-_\alpha + U_\alpha \tag{109}$$

in order to get the prediction $\hat{X}^-_\alpha[k+1]$. In this first step the odometrical measurements are used for a better evaluation of the applied control U_α.

2. Correction using visual data at time $(k+1)T$ in order to get the estimation $\hat{X}_\alpha[k+1]$.

This yields:

$$\hat{X}^-_\alpha[k+1] = \exp^{TA_\alpha}\hat{X}_\alpha[k] + \int_0^T \exp^{(T-s)A_\alpha} U_\alpha(kT+s)ds \tag{110a}$$

$$\hat{X}_\alpha[k+1] = \hat{X}^-_\alpha[k+1] + TD_\alpha\left(\alpha^v[k+1] - \hat{\alpha}^-[k+1]\right) \tag{110b}$$

with $U_\alpha = \begin{pmatrix} u^o_2 & 0\end{pmatrix}^T$ and $\hat{\alpha}^-[k+1] = \begin{pmatrix}1 & 0\end{pmatrix}\hat{X}^-_\alpha[k+1]$. From (18), a direct calculation gives

$$\forall t \in \mathbb{R}, \quad \exp^{tA_\alpha} = \begin{pmatrix}1 & -t\\ 0 & 1\end{pmatrix} \tag{111}$$

and the integral in (110a) becomes

$$\begin{aligned} I_\alpha &= \int_0^T \exp^{(T-s)A_\alpha} U_\alpha(kT+s)\,ds = \int_0^T \begin{pmatrix}1 & -(T-s)\\ 0 & 1\end{pmatrix}\begin{pmatrix}u^o_2(kT+s)\\ 0\end{pmatrix} ds\\ &= \begin{pmatrix}\int_0^T u^o_2(kT+s)ds\\ 0\end{pmatrix}\end{aligned}$$

From Equation (1),

$$\int_0^T u_2^o\,(kT+s)\,ds = \alpha_r\,[k+1] - \alpha_r\,[k] = \Delta\alpha_r^o[k+1] \tag{112}$$

so that, by (110a), (111), and (112),

$$\hat{X}_\alpha^-[k+1] = \begin{pmatrix} 1 & -T \\ 0 & 1 \end{pmatrix} \hat{X}_\alpha[k] + \begin{pmatrix} \Delta\alpha_r^o[k+1] \\ 0 \end{pmatrix} \tag{113}$$

Relations (113) and (110b) correspond precisely to (24b) and (25b).

E.1.2 p–estimator

We proceed as in the previous case. By using (111), one shows that the second component $\hat{c}^-(t)$ of the solution $\hat{X}_\alpha^-(t)$ to (109) is constant when $t \in [kT, (k+1)T)$, i.e. $\hat{c}^-(t) = \hat{c}[k]$. This implies that $A_p(\hat{c}^-(t))$ is also constant on this interval so that — compare with (110) —:

$$\hat{X}_p^-[k+1] = \exp^{T\hat{A}_p[k]}\,\hat{X}_p[k] + \int_0^T \exp^{(T-s)\hat{A}_p[k]}\,\hat{U}_p(kT+s)ds \tag{114a}$$

$$\hat{X}_p[k+1] = \hat{X}_p^-[k+1] + TD_p\left(p^v[k+1] - \hat{p}^-[k+1]\right) \tag{114b}$$

with $\hat{A}_p[k] \triangleq A_p(\hat{c}[k])$, $\hat{p}^-[k+1] = \begin{pmatrix} I_2 & 0 \end{pmatrix} \hat{X}_p^-[k+1]$ and

$$\hat{U}_p = \begin{pmatrix} u_1^o \cos\hat{\alpha}^- \\ u_1^o \sin\hat{\alpha}^- \\ 0 \\ 0 \end{pmatrix} \tag{115}$$

Let

$$J_2 = \begin{pmatrix} 0 & 1 \\ -1 & 0 \end{pmatrix}$$

so that, from (18),

$$A_p(c) = \begin{pmatrix} c\mathrm{J}_2 & -\mathrm{I}_2 \\ 0 & c\mathrm{J}_2 \end{pmatrix}$$

From the fact that $\mathrm{J}_2^2 = -\mathrm{I}_2$, one shows by induction that

$$\forall k > 0 \qquad A_p^{2k}(c) = \begin{pmatrix} c^{2k}\mathrm{J}_2^{2k} & 2k\,c^{2k-1}\mathrm{J}_2^{2k+1} \\ 0 & c^{2k}\mathrm{J}_2^{2k} \end{pmatrix}$$

$$\forall k \geq 0 \qquad A_p^{2k+1}(c) = \begin{pmatrix} c^{2k+1}\mathrm{J}_2^{2k+1} & (2k+1)\,c^{2k}\mathrm{J}_2^{2(k+1)} \\ 0 & c^{2k+1}\mathrm{J}_2^{2k+1} \end{pmatrix}$$

which yields

$$\exp^{tA_p(c)} = \sum_{k=0}^{\infty} \frac{(tA_p(c))^k}{k!}$$

$$\exp^{tA_p(c)} = \begin{pmatrix} \exp^{tc\mathrm{J}_2} & -t\exp^{tc\mathrm{J}_2} \\ 0 & \exp^{tc\mathrm{J}_2} \end{pmatrix} \tag{116}$$

Since $\hat{A}_p[k] = A_p(\hat{c}[k])$, we deduce from (116) that

$$\exp^{t\hat{A}_p[k]} = \begin{pmatrix} \exp^{t\hat{c}[k]\mathrm{J}_2} & -t\exp^{t\hat{c}[k]\mathrm{J}_2} \\ 0 & \exp^{t\hat{c}[k]\mathrm{J}_2} \end{pmatrix} \tag{117}$$

$$= \begin{pmatrix} R(-t\hat{c}[k]) & -tR(-t\hat{c}[k]) \\ 0 & R(-t\hat{c}[k]) \end{pmatrix} \tag{118}$$

From (115) and (118),

$$I[k+1] \triangleq \int_0^T \exp^{(T-s)\hat{A}_p[k]} \hat{U}_p\left(kT+s\right) ds = \begin{pmatrix} I_p[k+1] \\ 0 \\ 0 \end{pmatrix}$$

with

$$I_p[k+1] \triangleq \int_0^T u_1^o\left(kT+s\right) R\left(\left(s-T\right)\hat{c}[k]\right) \begin{pmatrix} \cos\hat{\alpha}^-\left(kT+s\right) \\ \sin\hat{\alpha}^-\left(kT+s\right) \end{pmatrix} ds$$

We have already shown in Section E.1.1 that, for $s \in [0,T]$,

$$\hat{\alpha}^-\left(kT+s\right) = \hat{\alpha}[k] - s\hat{c}[k] + \int_0^s u_2^o\left(kT+\tau\right) d\tau$$

therefore,

$$\hat{\alpha}^-[k+1] = \hat{\alpha}^-\left(kT+s\right) + \left(s-T\right)\hat{c}[k] + \int_s^T u_2^o\left(kT+\tau\right) d\tau$$

so that

$$I_p[k+1] = \int_0^T u_1^o\left(kT+s\right) \begin{pmatrix} \cos\left(\hat{\alpha}^-[k+1] - \int_s^T u_2^o\left(kT+\tau\right) d\tau\right) \\ \sin\left(\hat{\alpha}^-[k+1] - \int_s^T u_2^o\left(kT+\tau\right) d\tau\right) \end{pmatrix} ds \tag{119}$$

From Equation (1),

$$\int_s^T u_2^o\left(kT+\tau\right) d\tau = \alpha_r\left[k+1\right] - \alpha_r\left(kT+s\right) \tag{120}$$

and

$$\int_0^T \begin{pmatrix} u_1^o\left(kT+s\right)\cos\alpha_r\left(kT+s\right) \\ u_1^o\left(kT+s\right)\sin\alpha_r\left(kT+s\right) \end{pmatrix} ds = \begin{pmatrix} x_r\left[k+1\right] - x_r\left[k\right] \\ y_r\left[k+1\right] - y_r\left[k\right] \end{pmatrix} \tag{121}$$

We deduce from (119), (120), and (121), that

$$I_p[k+1] = R\left(\hat{\alpha}^-[k+1]\right) R\left(-\alpha_r\left[k+1\right]\right) \left(\begin{pmatrix} x_r \\ y_r \end{pmatrix}[k+1] - \begin{pmatrix} x_r \\ y_r \end{pmatrix}[k] \right)$$

Therefore

$$I[k+1] = \begin{pmatrix} R\left(\hat{\alpha}^-[k+1]\right)\Delta p_r^o\left[k+1\right] \\ 0 \\ 0 \end{pmatrix} \tag{122}$$

with

$$\Delta p_r^o\left[k+1\right] = R_{\alpha_r}[k+1] \left(\begin{pmatrix} x_r \\ y_r \end{pmatrix}[k+1] - \begin{pmatrix} x_r \\ y_r \end{pmatrix}[k] \right) \tag{123}$$

and where $R_{\alpha_r}[k+1]$ is the rotation matrix of angle $-\alpha_r[k+1]$ and x_r, y_r, and α_r are measured by odometry. Using (118), (122), and (123), (114a) becomes

$$\hat{X}_p^-[k+1] = \begin{pmatrix} R_c[k] & -TR_c[k] \\ 0 & R_c[k] \end{pmatrix} \hat{X}_p[k] + \begin{pmatrix} R_\alpha[k+1]\Delta p_r^o\left[k+1\right] \\ 0 \end{pmatrix} \tag{124}$$

with $R_c[k]$ the rotation matrix of angle $-T\hat{c}[k]$ and $R_\alpha[k+1]$ the rotation matrix of angle $\hat{\alpha}^-[k+1]$. Equations (124) and (114b) correspond precisely to (24a) and (25a).

E.2 Stability of the computed transverse function

From (27),

$$\|\Psi[k+1]\|^2 = \left(1+\beta\left(\|\Psi[k]\|^2-1\right)\right)^2\|\Psi[k]\|^2$$

Defining $\Delta_k \stackrel{\Delta}{=} \|\Psi[k]\|^2 - 1$, we have

$$\begin{aligned}\Delta_{k+1} &= (1+\beta\Delta_k)^2(\Delta_k+1)-1\\ &= (1+2\beta)\Delta_k + \beta(\beta+2)\Delta_k^2 + \beta^2\Delta_k^3\end{aligned}$$

so that $\Delta = 0$ is a locally asymptotically stable equilibrium point of this system provided that $\beta \in (-1,0)$. This is equivalent to the local asymptotic stability of $\|\Psi\| = 1$ for System (27).

F Stable equilibria of θ for straight-line longitudinal motion of the target

We assume here that the target is moving along a straight line with

$$u_t = (a,0,0)^T \quad , a \text{ constant and different from zero} \tag{125}$$

On the zero-dynamics $z \equiv 0$ — associated with the asymptotic stability of $z = 0$ — Equation (12) reduces to

$$\bar{u} = \begin{pmatrix} u_1 \\ u_2 \\ \dot{\theta}\end{pmatrix} = -H(\theta)^{-1}\begin{pmatrix}-a\\0\\0\end{pmatrix}$$

Therefore, from (9) and (10),

$$\begin{aligned}\dot{\theta} &= \begin{pmatrix}0 & 0 & 1\end{pmatrix}\bar{u}\\ &= \frac{\begin{pmatrix}0 & 0 & 1\end{pmatrix}}{\det H(\theta)}\begin{pmatrix}\frac{\varepsilon_1\varepsilon_2}{2}\cos(2\theta) & -\varepsilon_1\cos\theta & 0\\ -\varepsilon_2\sin(\varepsilon_2\cos\theta)\sin\theta & \cos(\varepsilon_2\cos\theta)\varepsilon_2\sin\theta & \det H(\theta)\\ \sin(\varepsilon_2\cos\theta) & -\cos(\varepsilon_2\cos\theta) & 0\end{pmatrix}\begin{pmatrix}a\\0\\0\end{pmatrix}\\ &= \frac{a\sin(\varepsilon_2\cos\theta)}{\det H(\theta)}\end{aligned}$$

Since $\varepsilon_2 \in (0,\pi/2]$ — in order to ensure that f is a transverse function — and since $a \neq 0$, the equilibria of the above differential equation are $\theta_0 = \pm\frac{\pi}{2}$. The linearization of this equation at any of these equilibria yields

$$\dot{\tilde{\theta}} \approx -\frac{a\varepsilon_2\cos(\varepsilon_2\cos\theta_0)\sin\theta_0}{\det H(\theta_0)}\tilde{\theta}$$

with $\tilde{\theta} \stackrel{\Delta}{=} \theta - \theta_e$, i.e.

$$\dot{\tilde{\theta}} \approx \begin{cases} -\frac{a\varepsilon_2}{\det H(\theta_0)}\tilde{\theta} & \text{if } \theta_0 = \frac{\pi}{2}\\ \frac{a\varepsilon_2}{\det H(\theta_0)}\tilde{\theta} & \text{if } \theta_0 = -\frac{\pi}{2}\end{cases}$$

Since, by (31), $\det H(\theta) < 0$ for any θ, one concludes that only

$$\theta_0 = -sign(a)\frac{\pi}{2}$$

is asymptotically stable on the zero dynamics.

References

[1] A. de Luca, G. Oriolo, and C. Samson. Feedback control of a nonholonomic car-like robot. In J.-P. Laumond, editor, *Robot motion planning and control*, volume 229 of *LNCIS*. Springer Verlag, 1998.

[2] W.E. Dixon, D.M. Dawson, E. Zergeroglu, and F. Zhang. Robust tracking and regulation control for mobile robots. *International Journal of Robust and Nonlinear Control*, 10:199–216, 2000.

[3] H. Kwakernaak and R. Sivan. *Linear Optimal Control Systems*. Wiley-Interscience, 1972.

[4] P. Morin and C. Samson. Practical stabilization of driftless systems on Lie groups. *IEEE Transactions on Automatic Control. To appear.*

[5] C. Samson. Control of chained systems. Application to path following and time-varying point-stabilization. *IEEE Trans. on Automatic Control*, 40:64–77, 1995.

[6] D.P. Tsakiris, K. Kapellos, C. Samson, P. Rives, and J.J. Borrelly. Experiments in real-time vision-based point stabilization of a nonholonomic mobile manipulator. In 5^{th} *Inter. Symp. on Exp. Rob.*, 1997.

Unité de recherche INRIA Sophia Antipolis
2004, route des Lucioles - BP 93 - 06902 Sophia Antipolis Cedex (France)

Unité de recherche INRIA Futurs : Parc Club Orsay Université - ZAC des Vignes
4, rue Jacques Monod - 91893 ORSAY Cedex (France)
Unité de recherche INRIA Lorraine : LORIA, Technopôle de Nancy-Brabois - Campus scienti£que
615, rue du Jardin Botanique - BP 101 - 54602 Villers-lès-Nancy Cedex (France)
Unité de recherche INRIA Rennes : IRISA, Campus universitaire de Beaulieu - 35042 Rennes Cedex (France)
Unité de recherche INRIA Rhône-Alpes : 655, avenue de l'Europe - 38334 Montbonnot Saint-Ismier (France)
Unité de recherche INRIA Rocquencourt : Domaine de Voluceau - Rocquencourt - BP 105 - 78153 Le Chesnay Cedex (France)

Éditeur
INRIA - Domaine de Voluceau - Rocquencourt, BP 105 - 78153 Le Chesnay Cedex (France)
http://www.inria.fr
ISSN 0249-6399